

AD-A032 066

AUBURN UNIV ALA ENGINEERING EXPERIMENT STATION
THE ANALYTICAL ANALYSIS OF A SINGLE POINT SUSPENSION TECHNIQUE --ETC(U)
AUG 76 J A SCHAEFFEL, J W REECE

F/G 16/4

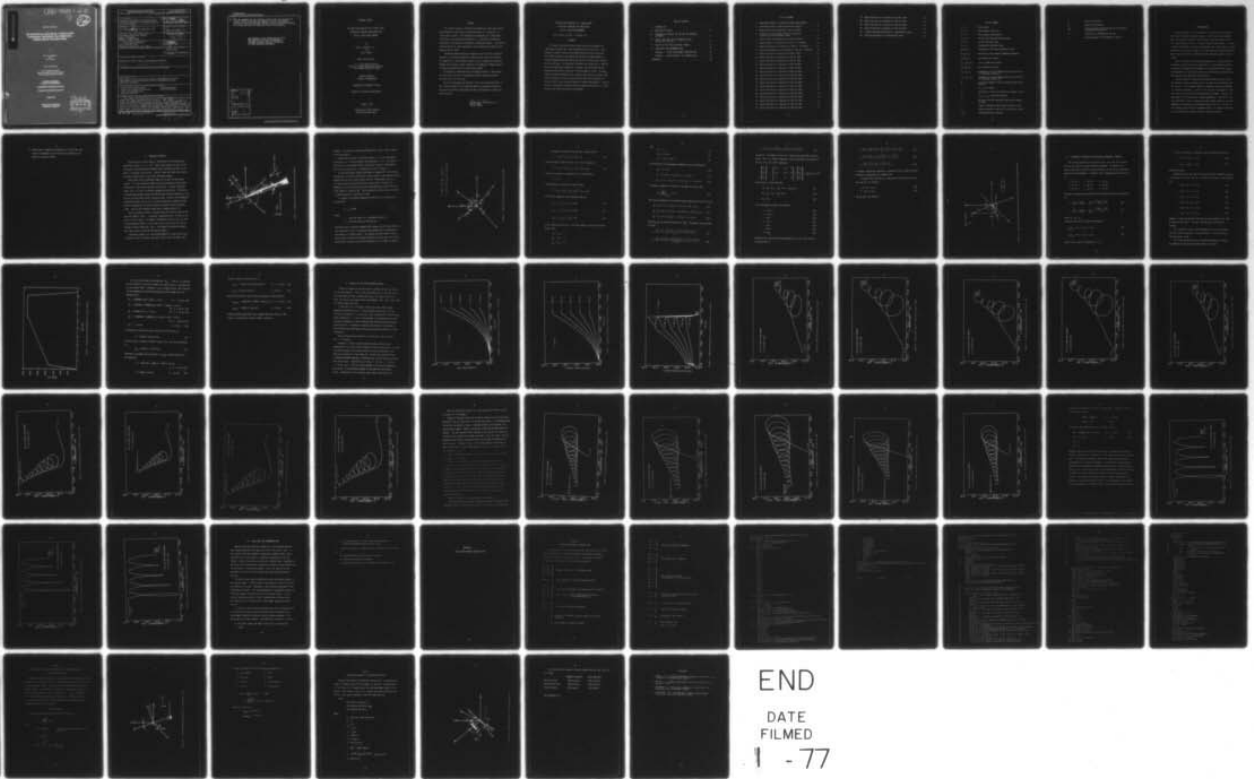
DAAG29-76-G-0060

UNCLASSIFIED

ARO-13651.1-AE

NL

1 of 1
ADA032066



END
DATE
FILMED
1 - 77

ARO-73651.1-A-E

[Handwritten signature]
12

AD A032066

TECHNICAL REPORT

**THE ANALYTICAL ANALYSIS OF A SINGLE POINT
SUSPENSION TECHNIQUE FOR PREDICTING
MISSILE THRUST MALALIGNMENT**

by

*John A. Schaeffel, Jr.
and
Joe W. Reece*

under contract with

U.S. Army Research Office
Research Triangle Park, North Carolina
Grant Number DAAG29-76-G-0060

**AUBURN UNIVERSITY
SCHOOL OF ENGINEERING
ENGINEERING EXPERIMENT STATION
Mechanical Engineering Department**

August 1976

Approved for Public Release
Distribution Unlimited

[Handwritten mark]
**DDC
RECEIVED
NOV 16 1976
B**

REPORT DOCUMENTATION PAGE		READ INSTRUCTIONS BEFORE COMPLETING FORM
1. REPORT NUMBER	2. GOVT ACCESSION NO.	3. RECIPIENT'S CATALOG NUMBER
4. TITLE (and Subtitle) The Analytical Analysis of a Single Point Suspension Technique for Predicting Missile Thrust Malalignment.		5. TYPE OF REPORT & PERIOD COVERED Final Report, 1 Oct 75 - 30 Sep 1976
7. AUTHOR(s) Joe W. Reece ¹⁰ John A. Schaeffel, Jr.		6. PERFORMING ORG. REPORT NUMBER
9. PERFORMING ORGANIZATION NAME AND ADDRESS Engineering Experiment Station Auburn University Auburn, Alabama 36830		8. CONTRACT OR GRANT NUMBER(s) DAAG29-76-G-0060 <i>new</i>
11. CONTROLLING OFFICE NAME AND ADDRESS U. S. Army Research Office Post Office Box 12211 Research Triangle Park, NC 27709		10. PROGRAM ELEMENT, PROJECT, TASK AREA & WORK UNIT NUMBERS 12 74 p.
14. MONITORING AGENCY NAME & ADDRESS (if different from Controlling Office)		12. REPORT DATE August 1976
		13. NUMBER OF PAGES 65
		15. SECURITY CLASS. (of this report) Unclassified
		15a. DECLASSIFICATION/DOWNGRADING SCHEDULE
16. DISTRIBUTION STATEMENT (of this Report) Approved for public release; distribution unlimited. 18 ARO 19 13651.1-AE		
17. DISTRIBUTION STATEMENT (of the abstract entered in Block 20, if different from Report)		
18. SUPPLEMENTARY NOTES The findings in this report are not to be construed as an official Department of the Army position, unless so designated by other authorized documents.		
19. KEY WORDS (Continue on reverse side if necessary and identify by block number) Missile Thrust Malalignment Initial Spin Rates Single Point Suspension Technique Spin Stabilization Lateral Perturbing Forces Rotational Dynamics		
20. ABSTRACT (Continue on reverse side if necessary and identify by block number) The lateral perturbine forces due to thrust malalignment can significantly affect the flight characteristics of a missile. Past attempts to predict thrust malalignment have not proven successful. This report proposes a new method for making valid measurements of the malalignment phenomena through the use of a single point tethered missile technique. The equations of motion for the missile in the test device are developed, coded into a computer and tested against well known exact analytical solutions for motion about a point. The mass, inertia and thrust equations for a typical test missile are then coded		

DD FORM 1 JAN 73 1473

EDITION OF 1 NOV 65 IS OBSOLETE
S/N 0102-014-6601

Unclassified
SECURITY CLASSIFICATION OF THIS PAGE (When Data Entered)

402 958

mt

Unclassified

SECURITY CLASSIFICATION OF THIS PAGE(When Data Entered)

20. into the computer and the resultant motion paths are simulated for various initial spin rates and degrees of thrust malalignment. Analysis of the collected data indicates that the tethered technique is a viable solution for predicting thrust malalignment.

THE FINDINGS IN THIS REPORT ARE NOT TO BE
CONSTRUED AS AN OFFICIAL DEPARTMENT OF
THE ARMY POSITION, UNLESS SO DESIGNATED
BY OTHER AUTHORIZED DOCUMENTS.

ACCESSION for		
NTIS	White Section	<input checked="" type="checkbox"/>
OCC	Staff Section	<input type="checkbox"/>
UNANNOUNCED		<input type="checkbox"/>
JUSTIFICATION		
BY		
DISTRIBUTION/AVAILABILITY CODES		
Dist.	AvAIL.	and/or SPECIAL
A		

SECURITY CLASSIFICATION OF THIS PAGE(When Data Entered)

TECHNICAL REPORT

THE ANALYTICAL ANALYSIS OF A SINGLE POINT
SUSPENSION TECHNIQUE FOR PREDICTING
MISSILE THRUST MALALIGNMENT

by

John A. Schaeffel, Jr.

and

Joe W. Reece

under contract with

U. S. Army Research Office
Research Triangle Park, North Carolina
Grant Number DAAG29-76-G-0060

AUBURN UNIVERSITY
SCHOOL OF ENGINEERING

ENGINEERING EXPERIMENT STATION

Mechanical Engineering Department

August, 1976

Approved for Public Release
Distribution Unlimited

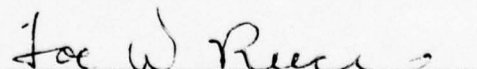
PREFACE

This report examines a technique for measuring rocket motor thrust malalignment by observing the associated motion of a tethered (at a single point) rocket. The technique was proposed by Mr. Tommy Howell of the Test and Evaluation Directorate, U. S. Army Missile Research, Development and Engineering Laboratory at Redstone Arsenal. The analysis reported herein has been supported by that Directorate through an Army Research Office grant.

The method examined here was proposed so as to utilize rotational dynamics as a response mechanism instead of more traditional methods of suspension for testing which usually yield a combination of motions. Indeed, most previous systems required a six-degree-of freedom analysis to relate observed motion to thrust malalignment.

We gratefully acknowledge the assistance of Messrs. Tommy Howell, Ted Haas and Leland Lee of the Redstone Arsenal who have provided technical data for this study.

We also acknowledge the editorial skill and extreme good humor of Mrs. Dianne Fretwell and Mr. Walter Clement of the Auburn University Mechanical Engineering Department who were indispensable in preparing the manuscript.



Joe W. Reece
Project Leader

THE ANALYTICAL ANALYSIS OF A SINGLE POINT
SUSPENSION TECHNIQUE FOR PREDICTING
MISSILE THRUST MALALIGNMENT

Joe W. Reece and John A. Scheffel, Jr.

ABSTRACT

The lateral perturbance forces due to thrust malalignment can significantly affect the flight characteristics of a missile. Past attempts to predict thrust malalignment have not proven successful. This report proposes a new method for making valid measurements of the malalignment phenomena through the use of a single point tethered missile technique. The equations of motion for the missile in the test device are developed, coded into a computer and tested against well known exact analytical solutions for motion about a point. The mass, inertia and thrust equations for a typical test missile are then coded into the computer and the resultant motion paths are simulated for various initial spin rates and degrees of thrust malalignment. Analysis of the collected data indicates that the tethered technique is a viable solution for predicting thrust malalignment.

TABLE OF CONTENTS

I. INTRODUCTION	1
II. EQUATIONS OF MOTION	5
III. INTEGRATION TECHNIQUE FOR SOLVING THE EQUATIONS OF MOTION	14
IV. THRUST, MASS AND INERTIA PARAMETERS FOR A TYPICAL TEST MISSILE	17
V. RESULTS OF TEST MISSILE MOTION STUDIES	21
VI. CONCLUSIONS AND RECOMMENDATIONS	48
APPENDIX I. THRUST MALALIGNMENT COMPUTER CODE	50
APPENDIX II. VERIFICATION OF THE COMPUTER CODE	59
REFERENCES	66

LIST OF FIGURES

1. Experimental Model for Predicting Thrust Malalignment	2
2. Coordinate System for Describing Missile Motion	6
3. Angular Velocities Expressed in the xyz System	8
4. Location of a Point Along a Missile's Spin Axis in the XYZ Inertia Reference Frame	13
5. Thrust Versus Time Relation for a Typical Missile	18
6. Nutation Angle as a Function of Time ($\dot{\phi} = 0$ rad/sec)	22
7. Nutation Velocity as a Function of Time ($\dot{\phi} = 0$ rad/sec)	23
8. Nutation Acceleration as a Function of Time ($\dot{\phi} = 0$ rad/sec)	24
9. Nozzle Position as a Function of Time (5-.001)	25
10. Nozzle Position as a Function of Time (5-.002)	26
11. Nozzle Position as a Function of Time (5-.003)	27
12. Nozzle Position as a Function of Time (5-.004)	28
13. Nozzle Position as a Function of Time (5-.005)	29
14. Nozzle Position as a Function of Time (10-.001)	31
15. Nozzle Position as a Function of Time (10-.002)	32
16. Nozzle Position as a Function of Time (10-.003)	33
17. Nozzle Position as a Function of Time (10-.004)	34
18. Nozzle Position as a Function of Time (10-.005)	35
19. Nozzle Position as a Function of Time (15-.001)	37
20. Nozzle Position as a Function of Time (15-.002)	38
21. Nozzle Position as a Function of Time (15-.003)	39
22. Nozzle Position as a Function of Time (15-.004)	40
23. Nozzle Position as a Function of Time (15-.005)	41
24. Nozzle Position as a Function of Time (S5-.001)	43

25. Nozzle Position as a Function of Time (S5-.002)	44
26. Nozzle Position as a Function of Time (S5-.003)	45
27. Nozzle Position as a Function of Time (S5-.004)	46
28. Nozzle Position as a Function of Time (S5-.005)	47
29. A Simple Pendulum Oscillating in a Gravitation Field	61
30. Spinning Gyroscope in a Gravitational Field	64

LIST OF SYMBOLS

ψ, θ, ϕ	Euler angles
$\dot{\psi}, \dot{\theta}, \dot{\phi}$	Euler angular velocities
$\ddot{\psi}, \ddot{\theta}, \ddot{\phi}$	Euler angular accelerations
x', y', z'	missile body fixed coordinate system
X, Y, Z	inertia reference frame
x, y, z	intermediate reference frame
H_x, H_y, H_z	components of the angular momentum vector
$\dot{H}_x, \dot{H}_y, \dot{H}_z$	derivatives of the angular momentum components
$\bar{e}_x, \bar{e}_y, \bar{e}_z$	xyz system unit vectors
$\bar{e}_{x'}, \bar{e}_{y'}, \bar{e}_{z'}$	x'y'z' system unit vectors
$\bar{e}_X, \bar{e}_Y, \bar{e}_Z$	XYZ system unit vectors
m_x, m_y, m_z	components of the net moment acting on the missile in coordinate system xyz
$m_{x'}, m_{y'}, m_{z'}$	components of the net moment acting on the missile in coordinate system x'y'z'
\bar{M}	gravitation moment in the xyz system acting on the missile
I	$I_{z'z'}$, roll inertia
\dot{I}	derivative of the roll inertia with respect to time
I'	$I_{x'x'} = I_{y'y'}$, transverse inertia
\dot{I}'	derivative of the transverse inertia with respect to time
$\bar{\Omega}$	angular velocity of the xyz set relative to XYZ
$\bar{\omega}$	angular velocity of the x'y'z' set relative to XYZ
g, G	acceleration due to gravity

m	mass of the missile
W	weight of the missile
\bar{R}_{gz}	position vector from the origin O to the center of gravity of the missile
\bar{V}	velocity of a differential mass dm
$\bar{\rho}$	position vector to a differential mass dm

I. INTRODUCTION

A major problem in missile dynamics is unpredictable flight path motion due to lateral perturbing forces. Thrust vector malalignment, which occurs when a missile's thrust vector is not coincidental with its' longitudinal spin axis, is often a cause of these forces. In order to reduce the effects of thrust malalignment, spin stabilization is often employed. The missile is given a spin rate about its' longitudinal axis which rotates the various perturbing forces and makes them less significant.

Since the effects of thrust malalignment are a serious problem in achieving a specified missile flight path, it is desirable to be able to measure the degree of malalignment in a particular missile system. The knowledge thus gained can be used to correct design characteristics and produce better downrange flight motions.

Various attempts to measure thrust malalignment have been made. The techniques which have been used in the past have not produced useful results. A new proposed method for measuring thrust malalignment is indicated in Figure 1. A missile for testing is suspended in a ball and socket joint which allows three degrees of freedom. The spin and main motors of the missile are started sequentially. The missile may be constrained initially as desired to give uniform starting conditions. Depending on the amount of malalignment and initial spin, the missile will undergo some particular subsequent motion. A circular constraint ring is provided to prevent excessive lateral excursions.

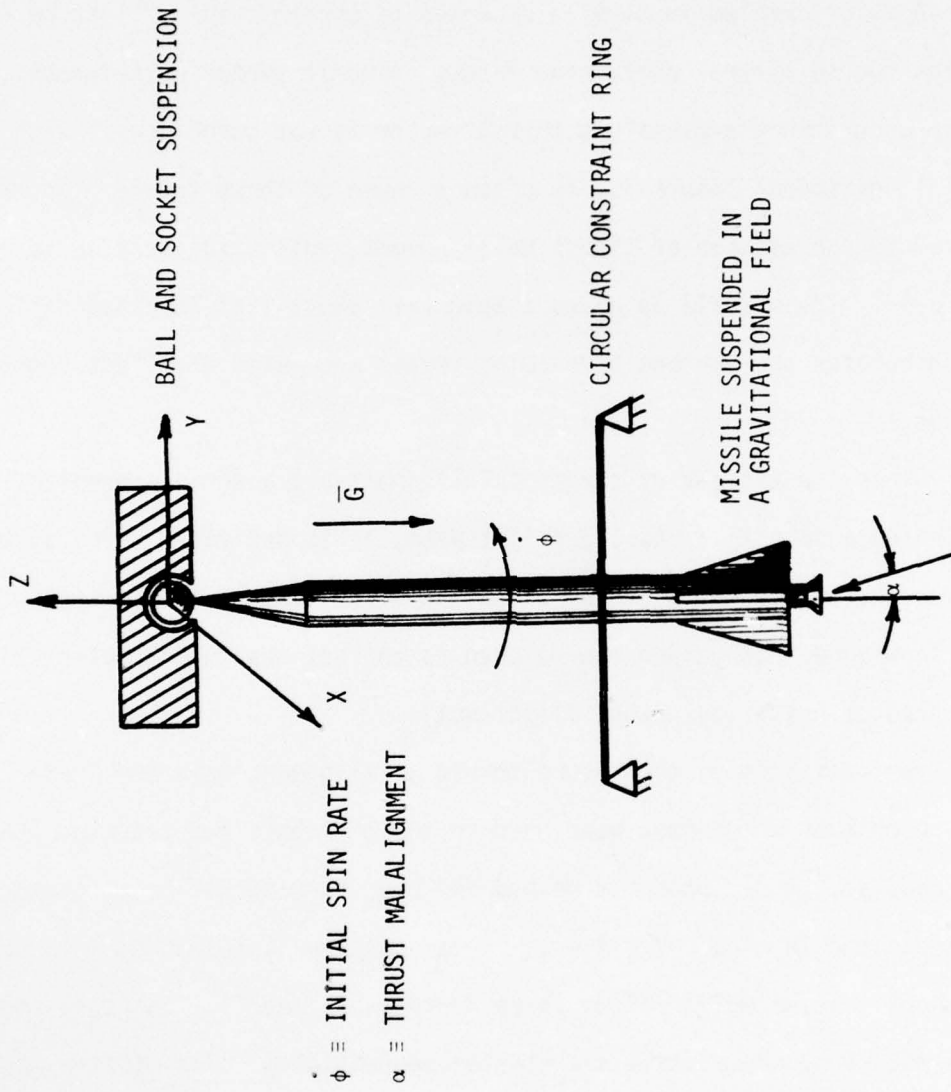


Figure 1. Experimental Model for Predicting Thrust Malalignment

The objective of this report is to predict the motion of a test missile, in the constraining fixture, with known inertia, mass, and thrust characteristics for various degrees of thrust malalignment and initial spin rates. The parameters describing the motion of the missile are displayed at the end and may serve as a set of prediction curves for actual testing. If one measures the motion of a real missile in the test fixture, the curves may be used to relate the degree of thrust malalignment. The results given here can also be used as a basis for further consideration for this method of testing.

The results of this analysis show that this testing method may be a viable way to measure thrust malalignment. Excursions predicted for a typical rocket are within the measurable range and do not take the rocket into unreasonable motion patterns. Also, some surprising results occur which shed some light on the necessary spin rate required for the stabilization of rockets.

The analysis involves five steps:

1. Development of the equations of motion for the constrained missile.
2. Development of a technique for solving the equations of motion.
3. Testing of the solution technique against known exact solutions (Appendix II).
4. Establishment of the basic characteristics for a typical test missile. These characteristics will include mass, inertia, and thrust equations as a function of time.

5. Coding into a computer the equations in (4) for the test missile to generate a set of curves for predicting its' motion in the test fixture.

II. EQUATIONS OF MOTION

The motion of a missile about a fixed point can be described by three Euler angles, ψ , θ , ϕ , [1]. These three angles are used to give the spatial interrelationship between three coordinate systems, one of which is attached to the missile. Figure 2 shows the three Euler angles and their relationship to the three coordinate systems.

The primary inertia reference frame will be the XYZ coordinate system. It is the reference frame from which an observer would record the motion of the missile relative to the earth. A second reference frame, the $x'y'z'$ set, is rigidly attached to the missile. The forces and associated moments along with the mass and inertia properties of the missile are described by this reference frame. Finally, an intermediate coordinate system, the xyz set, is used to relate the location of the missile longitudinal spin axis relative to the XYZ inertia reference frame. Each of the reference frames have a common origin at 0.

The xyz reference frame is related to the XYZ inertia frame by the two Euler angles ψ and θ . In general, coordinate axis x of the xyz set moves in the XY plane. Its angular relationship to the X axis is given by the precession angle ψ . Also, the y and z axis of the xyz set are allowed to rotate about the x axis. The angular relationship between the Z and z axes is given by the nutation angle θ .

Coordinate system $x'y'z'$ may be described by a single Euler angle ϕ relative to the xyz frame, since the z and z' axes are always coin-

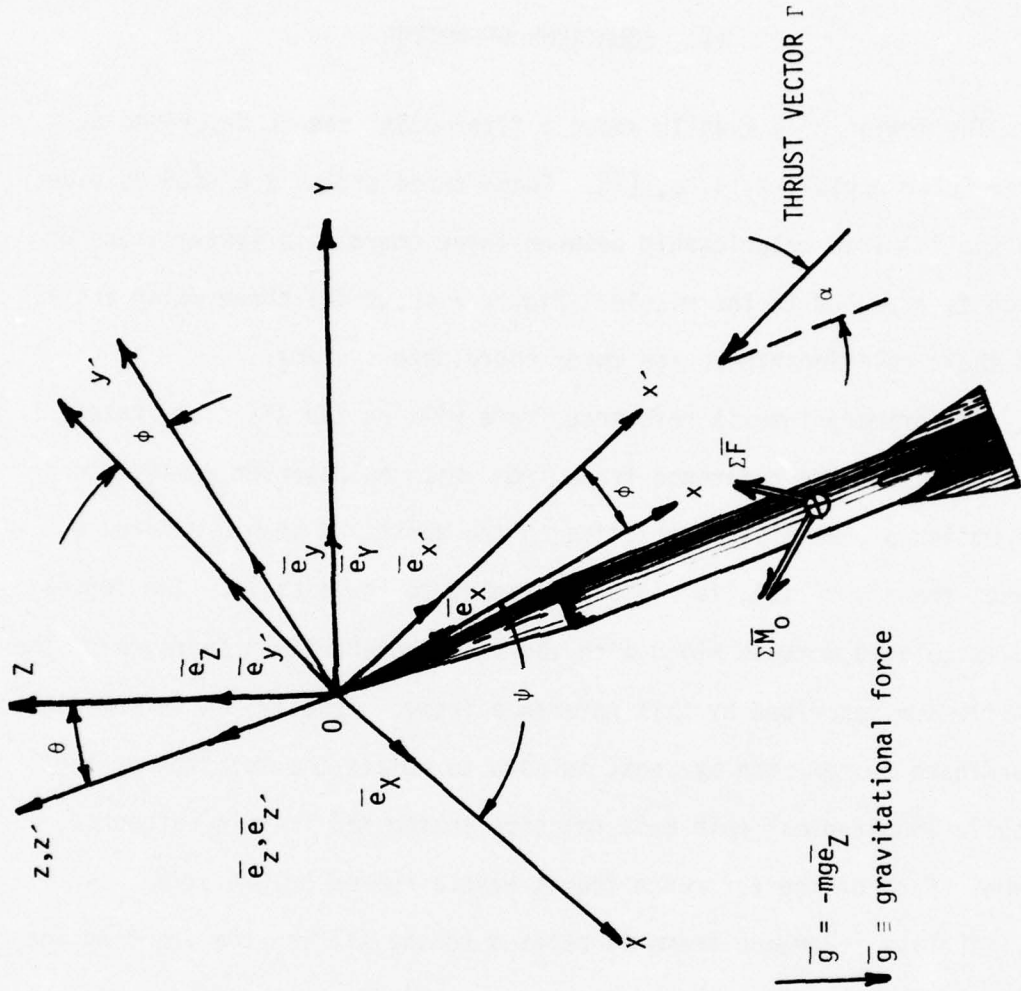


Figure 2. Coordinate System for Describing Missile Motion

cidental. The angular relationship between the x and x' axes is given by the spin angle ϕ .

Associated with each of the Euler angles ψ , θ , ϕ are the angular velocities $\dot{\psi}$, $\dot{\theta}$, $\dot{\phi}$ and the angular accelerations $\ddot{\psi}$, $\ddot{\theta}$, $\ddot{\phi}$. The nose of the missile is considered fixed at the origin O and its' longitudinal spin axis lies along the $-z'$ coordinate axis as in Figure 2.

For the coordinate systems described, the degree of missile thrust malalignment is given by the angle α [rad.], which is the angular measure between the missile's thrust vector and its' longitudinal spin axis. The total force acting on the missile at any time is given by $\Sigma \bar{F}$. Moments due to the various forces are taken about the origin O and the total moment is given by $\Sigma \bar{M}_O$. The direction of the force due to gravity is taken along the $-Z$ axis for all time.

In general, the angular momentum of the missile is given by the relation [2]:

$$\bar{H} = \int_b \bar{\rho} \times \bar{V} dm \quad (1)$$

where,

$\bar{\rho} \equiv$ position vector to a differential mass dm

$\bar{V} \equiv$ velocity vector of the mass dm .

Since the missile maintains symmetry with respect to its' mass distribution along the z' axis, a principle axes problem exist and therefore, the products of inertia vanish. The angular velocity vectors $\bar{\Omega}$ and $\bar{\omega}$ may be used to describe the angular motions of the xyz and $x'y'z'$ sets, respectively, relative to the XYZ coordinate set, as shown in Figure 3.

$$\bar{\Omega} = \dot{\theta} \bar{e}_x + \dot{\psi} \sin \theta \bar{e}_y + \dot{\psi} \cos \theta \bar{e}_z$$

$$\bar{\omega} = \dot{\theta} \bar{e}_x + \dot{\psi} \sin \theta \bar{e}_y + (\dot{\phi} + \dot{\psi} \cos \theta) \bar{e}_z$$

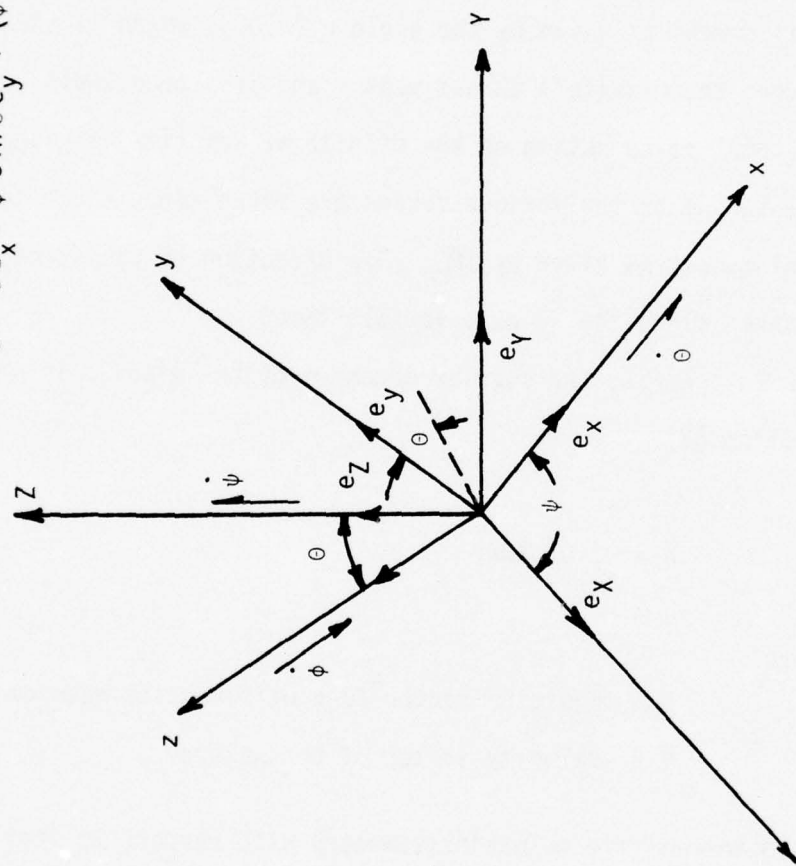


Figure 3. Angular Velocities Expressed in the xyz System

The angular velocity of the xyz set is given by [1]:

$$\bar{\omega} = \dot{\theta} \bar{e}_x + \dot{\psi} \sin \theta \bar{e}_y + \dot{\psi} \cos \theta \bar{e}_z \quad (2)$$

and the angular velocity of the x'y'z' set is given by:

$$\bar{\omega} = \dot{\theta} \bar{e}_x + \dot{\psi} \sin \theta \bar{e}_y + (\dot{\phi} + \dot{\psi} \cos \theta) \bar{e}_z \quad (3)$$

Since the velocity \bar{V} in equation (1) is specified by:

$$\bar{V} = \bar{\omega} \times \bar{\rho}$$

and there are no products of inertia, then,

$$\bar{H} = I_{x'x'} \omega_x \bar{e}_x + I_{y'y'} \omega_y \bar{e}_y + I_{z'z'} \omega_z \bar{e}_z$$

The inertia components are therefore given as,

$$I_{x'x'} = \int_{\beta} (\rho_{y'}^2 + \rho_{z'}^2) dm \quad (4)$$

$$I_{y'y'} = \int_{\beta} (\rho_{z'}^2 + \rho_{x'}^2) dm \quad (5)$$

$$I_{z'z'} = \int_{\beta} (\rho_{x'}^2 + \rho_{y'}^2) dm \quad (6)$$

Since, symmetry along the z' axis with respect to mass distribution exists, then:

$$I_{zz} = I_{z'z'} = I$$

$$I_{xx} = I_{x'x'} = I'$$

$$I_{yy} = I_{y'y'} = I'$$

and,

$$H_x = I'\dot{\theta}' \quad (7)$$

$$H_y = I'\dot{\psi} \sin \theta \quad (8)$$

$$H_z = I(\dot{\phi} + \dot{\psi} \cos \theta) \quad (9)$$

The derivative of the momentum components may be expressed as:

$$\dot{H}_x = \dot{I}'\dot{\theta}' + I'\ddot{\theta}' \quad (10)$$

$$\dot{H}_y = \dot{I}'\dot{\psi} \sin \theta + I'\ddot{\psi} \sin \theta + I'\dot{\psi} \dot{\theta}' \cos \theta \quad (11)$$

$$\dot{H}_z = \dot{I}(\dot{\phi} + \dot{\psi} \cos \theta) + I(\ddot{\phi} + \ddot{\psi} \cos \theta - \dot{\psi} \dot{\theta}' \sin \theta) \quad (12)$$

The general equation of motion for the body is given as [2]:

$$\bar{m} = \left\{ \frac{d\bar{H}}{dt} \right\}_{xyz} + \bar{\omega} \times \bar{H} \quad (13)$$

The scalar components of the moment vector equations given by (13) are:

$$M_x = \dot{I}'\dot{\theta}' + I'\ddot{\theta}' + I\dot{\phi}\dot{\psi} \sin \theta + (I-I')\dot{\psi}^2 \sin \theta \cos \theta \quad (14)$$

$$M_y = \dot{I}'\dot{\psi} \sin \theta + I'\ddot{\psi} \sin \theta + 2I'\dot{\psi}\dot{\theta}' \cos \theta - I\dot{\theta}'(\dot{\phi} + \dot{\psi} \cos \theta) \quad (15)$$

$$M_z = \dot{I}(\dot{\phi} + \dot{\psi} \cos \theta) + I\ddot{\phi} + I\ddot{\psi} \cos \theta - I\dot{\psi}\dot{\theta}' \sin \theta + I\dot{\psi} \dot{\theta}' \cos \theta \quad (16)$$

where M_x , M_y , M_z are the components of $\Sigma \bar{M}_0$. The angular accelerations are then:

$$\ddot{\theta}' = \frac{M_x - \dot{I}'\dot{\theta}' - I\dot{\phi}\dot{\psi} \sin \theta - (I-I')\dot{\psi}^2 \sin \theta \cos \theta}{I'} \quad (17)$$

$$\ddot{\psi} = \frac{M_y - \dot{I}'\dot{\psi} \sin \theta - 2I'\dot{\psi}\dot{\theta}' \cos \theta + I\dot{\theta}'(\dot{\phi} + \dot{\psi} \cos \theta)}{I' \sin \theta} \quad (18)$$

$$\ddot{\phi} = \frac{M_z - I \dot{\phi} - I \dot{\psi} \cos \theta - I \ddot{\psi} \cos \theta + I \dot{\psi} \dot{\theta} \sin \theta}{I} \quad (19)$$

In general, the moments in the x'y'z' body fixed coordinate system are known. The x'y'z' moment components can be transformed into moments in the xyz set by the matrix operation:

$$\begin{bmatrix} M_x \\ M_y \\ M_z \end{bmatrix} = \begin{bmatrix} \cos \phi & -\sin \phi & 0 \\ \sin \phi & \cos \phi & 0 \\ 0 & 0 & 1 \end{bmatrix} \cdot \begin{bmatrix} M_{x'} \\ M_{y'} \\ M_{z'} \end{bmatrix} + \omega R_{gz} \sin \theta \Big|_x \quad (20)$$

which results in the relations:

$$M_x = M_{x'} \cos \phi - M_{y'} \sin \phi + \omega R_{gz} \sin \theta \quad (21)$$

$$M_y = M_{x'} \sin \phi + M_{y'} \cos \phi \quad (22)$$

$$M_z = M_{z'} \quad (23)$$

If the following variables are defined:

$$v = \dot{\psi} \cos \theta \quad (24)$$

$$\lambda = \psi \sin \theta \quad (25)$$

$$\beta = \cos \theta \quad (26)$$

$$\mu = \sin \theta \quad (27)$$

$$\epsilon = \cos \phi \quad (28)$$

$$\rho = \sin \phi \quad (29)$$

$$m = \omega R_{gz} \quad (30)$$

Equations (21) through (30) and equations (17), (18), and (19) may be simplified to:

$$\ddot{\theta} = \frac{M_{x'} \epsilon - M_{y'} \rho + m\mu - \dot{I}' \dot{\theta} + (I'v - I(\dot{\phi} + v)) \lambda}{I'} \quad (31)$$

$$\ddot{\psi} = \frac{M_{x'} \rho + M_{y'} \epsilon - \dot{I}' \lambda + (I(\dot{\phi} + v) - 2I'v) \dot{\theta}}{I' \mu} \quad (32)$$

$$\ddot{\phi} = \frac{M_{z'} - \dot{I}'(\dot{\phi} + v) - I(\ddot{\psi} - \dot{\theta}\lambda)}{I} \quad (33)$$

A suitable integration technique is required to solve these nonlinear differential equations (31) through (33).

To predict the location of a fixed point along the spin axis of the missile, the relations:

$$X = R \sin \theta \sin \psi \quad (34)$$

$$Y = -R \sin \theta \cos \psi \quad (35)$$

may be used, see Figure 4.

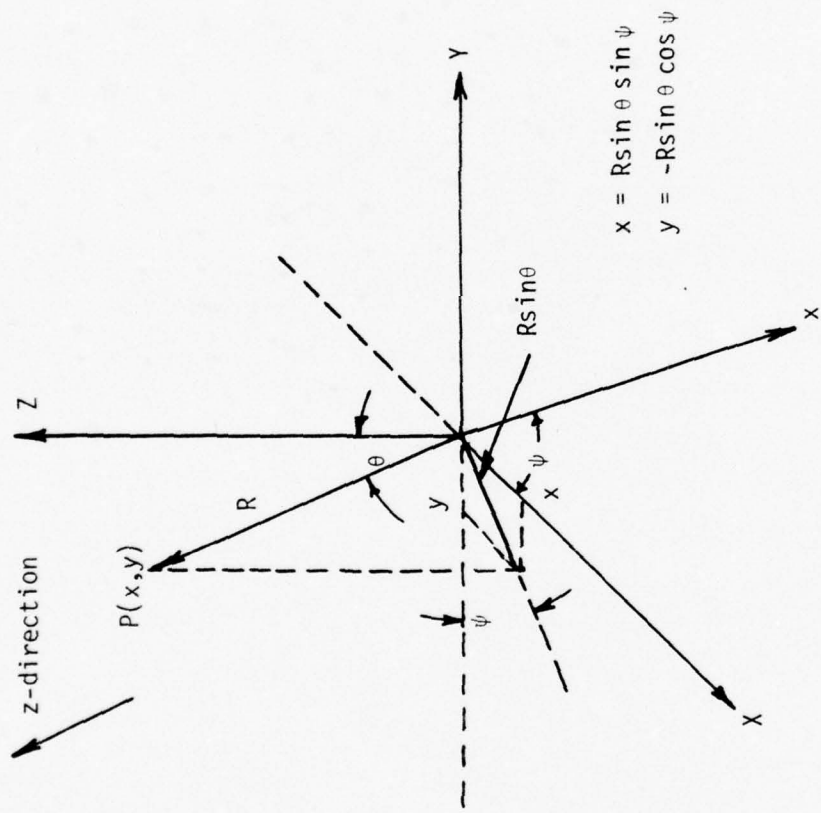


Figure 4. Location of a Point A Missile's Spin Axis in the XYZ Inertia Reference Frame

III. INTEGRATION TECHNIQUE FOR SOLVING THE EQUATIONS OF MOTION

The solution algorithm for equations (31), (32), and (33) involves the use of a numerical forward marching technique. In general, the angular positions, velocities and accelerations of the various coordinate systems are time dependent. Therefore, their components may be expressed as:

$$\begin{aligned} \ddot{\psi} &= f_1(t) ; & \dot{\psi} &= f_2(t) ; & \psi &= f_3(t) \\ \ddot{\theta} &= g_1(t) ; & \dot{\theta} &= g_2(t) ; & \theta &= g_3(t) \\ \ddot{\phi} &= h_1(t) ; & \dot{\phi} &= h_2(t) ; & \phi &= h_3(t) \end{aligned}$$

Consider the precession acceleration and velocity which may be expressed as:

$$\ddot{\psi} = \lim_{\Delta t \rightarrow 0} \frac{\Delta \dot{\psi}(t)}{\Delta t} = \lim_{\Delta t \rightarrow 0} \frac{\dot{\psi}(t_2) - \dot{\psi}(t_1)}{\Delta t} \quad (36)$$

$$\dot{\psi} = \lim_{\Delta t \rightarrow 0} \frac{\Delta \psi(t)}{\Delta t} = \lim_{\Delta t \rightarrow 0} \frac{\psi(t_2) - \psi(t_1)}{\Delta t} \quad (37)$$

where $\Delta t = t_2 - t_1$.

Equations (36) and (37) may be rewritten as:

$$\lim_{\Delta t \rightarrow 0} \ddot{\psi} \Delta t = \dot{\psi}(t_2) - \dot{\psi}(t_1) \quad (38)$$

$$\lim_{\Delta t \rightarrow 0} \dot{\psi} \Delta t = \psi(t_2) - \psi(t_1) \quad (39)$$

where $\ddot{\psi}$ and $\dot{\psi}$ may be evaluated at $t = t_1$.

As the time interval Δt decreases, the approximations given by:

$$\ddot{\psi}_1 \Delta t = \dot{\psi}(t_2) - \dot{\psi}(t_1) \quad (40)$$

$$\dot{\psi}_1 \Delta t = \psi(t_2) - \psi(t_1) \quad (41)$$

become more exact.

Equations such as (40) and (41) may be coded for computed solutions to equations (31), (32), and (33). The basic relations for the computer are:

$$\dot{\psi}(t_2) = \ddot{\psi}_1 \Delta t + \dot{\psi}(t_1) \quad (42)$$

$$\psi(t_2) = \dot{\psi}_1 \Delta t + \psi(t_1) \quad (43)$$

$$\dot{\theta}(t_2) = \ddot{\theta}_1 \Delta t + \dot{\theta}(t_1) \quad (44)$$

$$\theta(t_2) = \dot{\theta}_1 \Delta t + \theta(t_1) \quad (45)$$

$$\dot{\phi}(t_2) = \ddot{\phi}_1 \Delta t + \dot{\phi}(t_1) \quad (46)$$

$$\phi(t_2) = \dot{\phi}_1 \Delta t + \phi(t_1) \quad (47)$$

Appendix I gives the computer code used to solve equations (31)-(33) by equations (42)-(47). The basic solution may be outlined as follows:

(1) Establish initial missile parameters such as orientation, mass and inertia properties. Also establish $t = 0$ as the solution starting point in time.

(2) Given the existing set of spatial constraints, calculate the moments acting upon the missile about the origin 0.

(3) Solve for the new angular acceleration components of the reference frames using equations (31), (32), and (33).

(4) Solve for the new angular position components of the reference frames using equations (43), (45), and (47).

(5) Solve for the new angular velocity components of the reference frames using equations (42), (44), and (46).

(6) Increment the time variable of the solution by ΔT and check to see if the elapsed time is greater than the time requested for the solution. If the elapsed time is less than the time requested, go to step (2). Also, print out any results obtained. If the elapsed time has exceeded the time requested for the solution, end the program.

IV. THRUST, MASS AND INERTIA PARAMETERS
FOR A TYPICAL TEST MISSILE

For investigating the motion of a typical missile system, a set of test parameters for thrust, mass and inertia properties have been developed. Figure 5 shows the thrust versus time relation for a missile under investigation. The thrust simulation consists of four linear segments which comprise four special time phases of the burning process. These relations may be expressed as follows:

$$\text{Thrust} = 300000t \text{ (lb)} \quad 0 \leq t \leq .05 \text{ sec} \quad (48)$$

$$\text{Thrust} = 18333.33t + 14000 \text{ (lb)} \quad .05 \leq t \leq .65 \text{ sec} \quad (49)$$

$$\text{Thrust} = 26000 \text{ (lb)} \quad .65 \leq t \leq .90 \text{ sec} \quad (50)$$

$$\text{Thrust} = -520000t + 494000 \text{ (lb)} \quad .90 \leq t \leq .95 \text{ sec} \quad (51)$$

$$\text{Thrust} = 0 \text{ (lb)} \quad t \geq .95 \text{ sec} \quad (52)$$

The time dependent thrust relations can be used to generate a set of moments about the origin 0 in the x'y'z' coordinate set. If α is defined as the thrust malalignment angle, measured in radians, then the moment relations acting upon the missile may be given as:

$$M_{x'} = -R_{tx'} \sin \left[\frac{\text{Thrust} (\alpha)}{26000} \right] \text{Thrust (in-lb)} \quad (53)$$

$$M_{y'} = 0 \text{ (in-lb)} \quad (54)$$

$$M_{z'} = 0 \text{ (in-lb)} \quad (55)$$

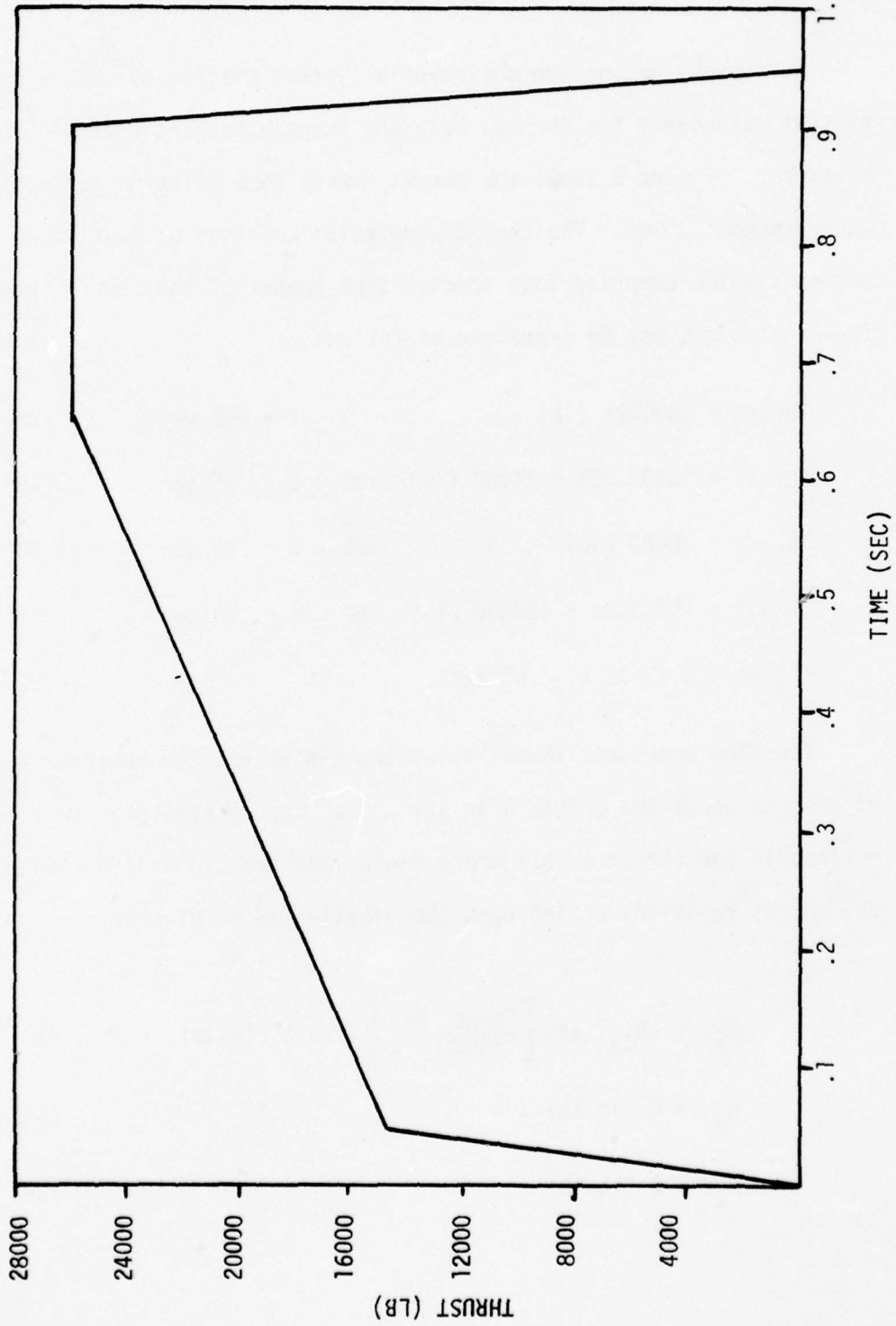


Figure 5. Thrust Versus Time Relation for a Typical Missile

For the missile under investigation, $-R_{tx}$, = -135 in., is defined as the location on the missile where the thrust vector is considered to act as a point force. Therefore, a set of moment versus time relations can be developed by substituting equations (48) through (52) into equation (53):

$$M_{x_1} = 40500000t \sin(11.538t\alpha) \quad (\text{in-lb}) \quad 0 \leq t \leq .05 \text{ sec} \quad (56)$$

$$M_{x_1} = (2475000t + 1890000)\sin((.7051t + .5385)\alpha) \quad (\text{in-lb}) \\ .05 \leq t \leq .65 \text{ sec} \quad (57)$$

$$M_{x_1} = 3510000 \sin(\alpha) \quad (\text{in-lb}) \quad .65 \leq t \leq .90 \text{ sec} \quad (58)$$

$$M_{x_1} = (-70200000t + 66690000) \sin((-20t + 19)\alpha) \quad (\text{in-lb}) \\ .90 \leq t \leq .95 \text{ sec} \quad (59)$$

$$M_{x_1} = 0 \quad (\text{in-lb}) \quad t \geq .95 \text{ sec} \quad (60)$$

The weight of the missile varies because of fuel burn-up as,

$$w = -87.589t + 250.19 \quad (\text{lbs}) \quad (61)$$

and the center of gravity location in the x'y'z' set can be expressed as:

$$R_{gz} = 14.3011t - 61.518 \quad (\text{in}) \quad (62)$$

Therefore, the moment due to gravity, $M = R_{gz}w$, varies according to the equations,

$$M = -1252.619t^2 + 8966.3t - 15391.2 \quad (\text{in-lb}) \\ 0 \leq t \leq .95 \text{ sec} \quad (63)$$

$$M = -8003.7 \quad (\text{in-lb}) \quad t \geq .95 \text{ sec} \quad (64)$$

The roll inertia of the missile is

$$I_{\text{roll}} = -14.614t + 43.155 \text{ (slug-in}^2\text{)} \quad 0 \leq t \leq .95 \text{ sec} \quad (65)$$

$$I_{\text{roll}} = 29.271 \text{ (slug-in}^2\text{)} \quad t \geq .95 \text{ sec} \quad (66)$$

While the transverse inertia varies according to the equations,

$$I_{\text{trans.}} = -22428.59t + 39196.2 \text{ (slug-in}^2\text{)} \quad 0 \leq t \leq .95 \text{ sec} \quad (67)$$

$$I_{\text{trans.}} = 17889.75 \text{ (slug-in}^2\text{)} \quad t \geq .95 \text{ sec} \quad (68)$$

Equations (56) through (60), (63) through (68) were coded into the computer to produce the results shown in section V.

V. RESULTS OF TEST MISSILE MOTION STUDIES

Figures 6 through 23 are the result of coding the data in section IV into the computer. Four initial spin rates of 0, 5, 10, and 15 rps (rev/sec) were utilized in making the plots. For each initial spin rate, five values of maximum thrust malalignment, .001, .002, .003, .004, and .005 radians were used.

In the case of $\dot{\phi} = 0$ rad/sec initial spin rate, the nutation components consisting of θ , $\dot{\theta}$, $\ddot{\theta}$ were plotted versus time. For the initial spin rates of $\alpha = 5, 10, \text{ and } 15$ rps, the position of the missile nozzle located at $z' = -135$ in. was plotted in XY coordinates with the functional parameter of time indicating the starting and ending points of the solution. An observer located at the origin-0,--see Figure 2, and recording each event would notice the given nozzle patterns in the z-direction.

Test (a) Thrust Malalignment of a Test Missile with no Initial Spin, $\dot{\phi} = 0$ rev/sec.

Figures 6, 7, and 8 give the nutation angle, velocity, and acceleration of the test missile without an initial spin rate ($\dot{\phi} = 0$ rps). The various stages of the thrust process are easily observed in the nutration acceleration, (see Figure 8). As the rate at which thrust is generated changes abruptly, discontinuities in the nutation acceleration curves occur. Specifically, at times $t = .05$ sec, $t = .65$ sec, $t = .90$ sec, and $t = .95$ sec, abrupt changes in the thrust generation rate result in discontinuous changes in the nutation acceleration curves. Observation of the nutation angle versus time curve (see

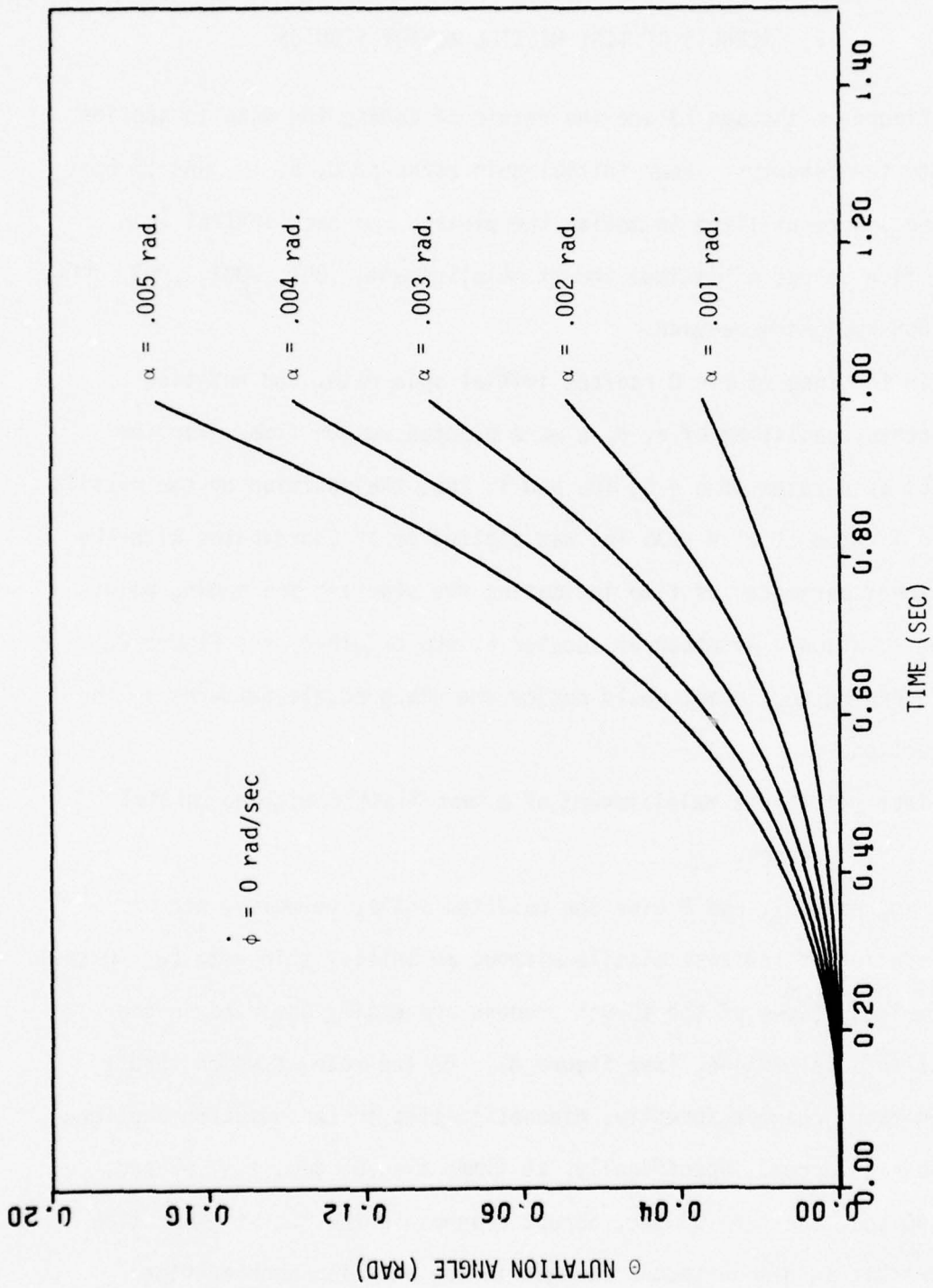


Figure 6. Nutation Angle as a Function of Time ($\dot{\phi} = 0$ rad/sec)

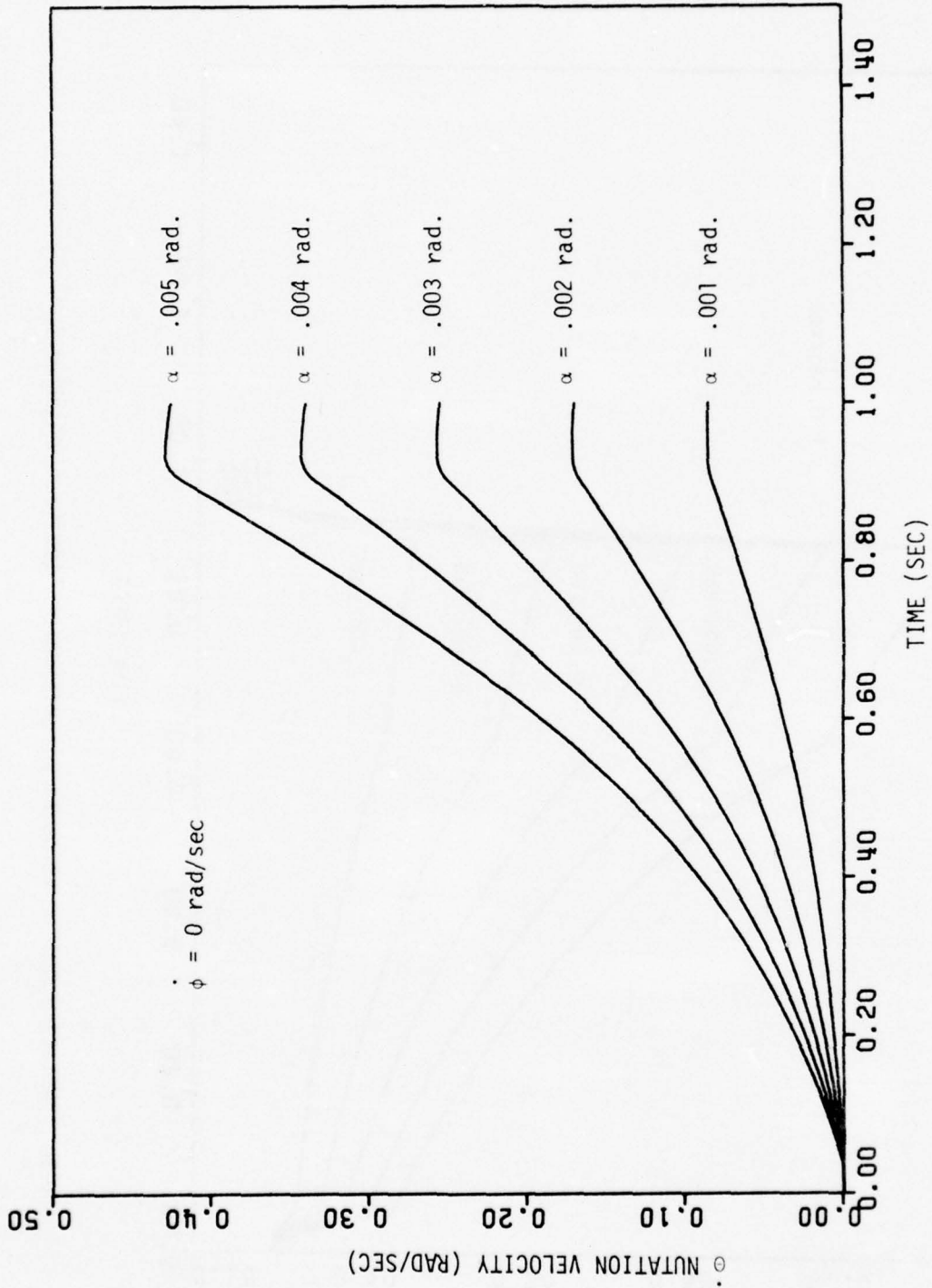


Figure 7. Nutation Velocity as a Function of Time ($\dot{\phi} = 0$ rad/sec)

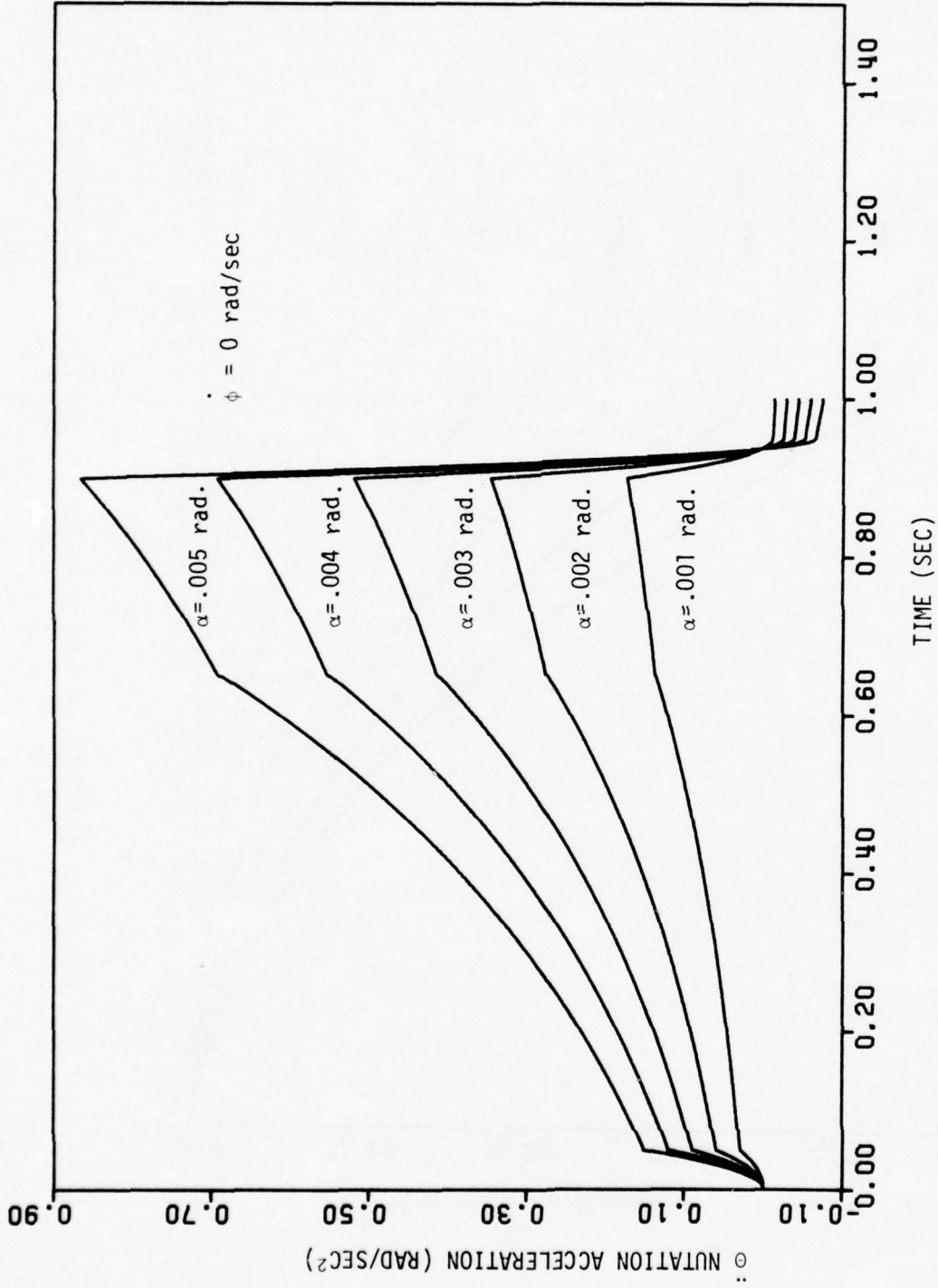


Figure 8. Nutation Acceleration as a Function of Time ($\dot{\phi} = 0 \text{ rad/sec}$)

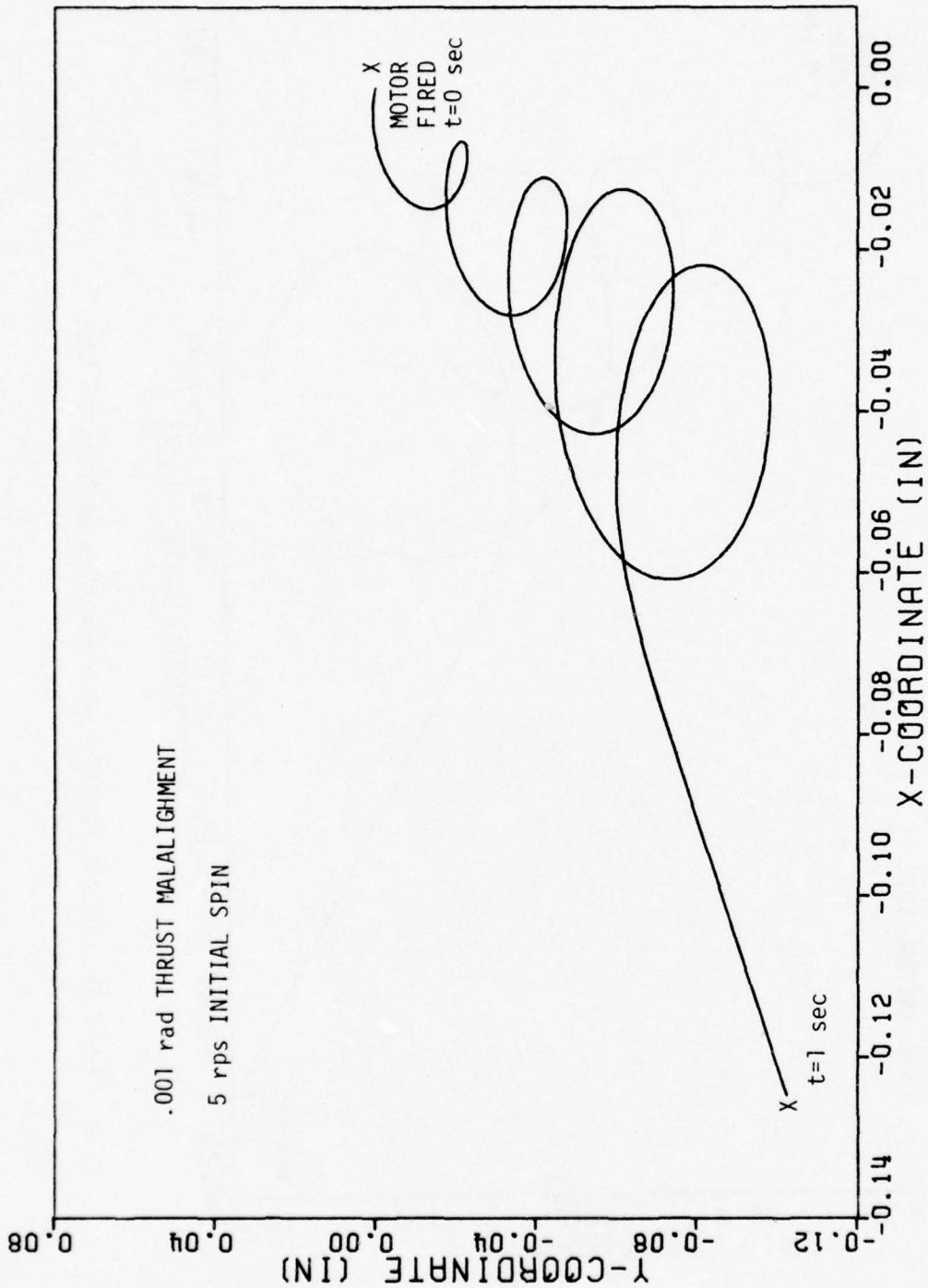


Figure 9. Nozzle Position as a Function of Time (5-.001)

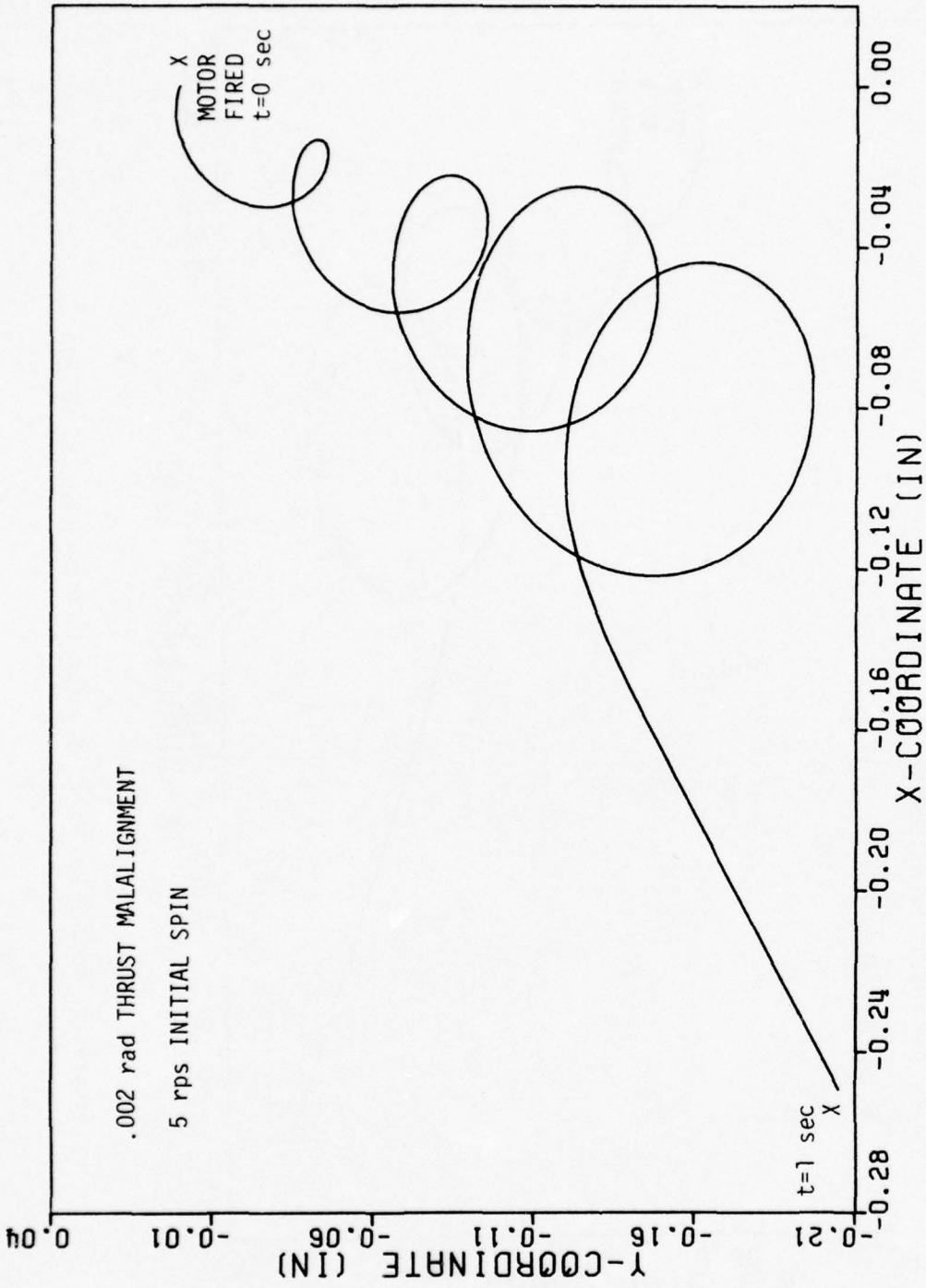


Figure 10. Nozzle Position as a Function of Time (5-.002)

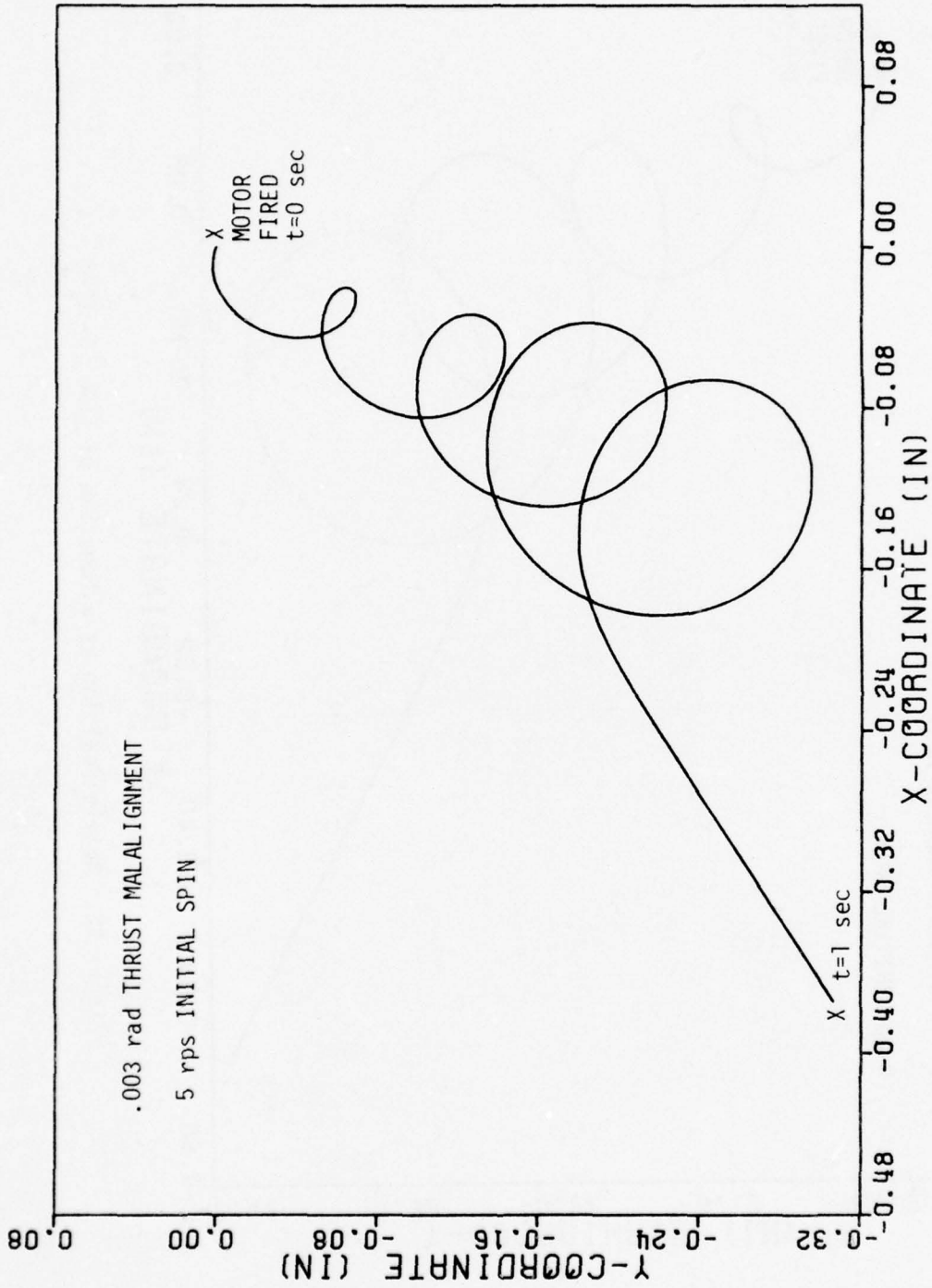


Figure 11. Nozzle Position as a Function of Time (5-.003)

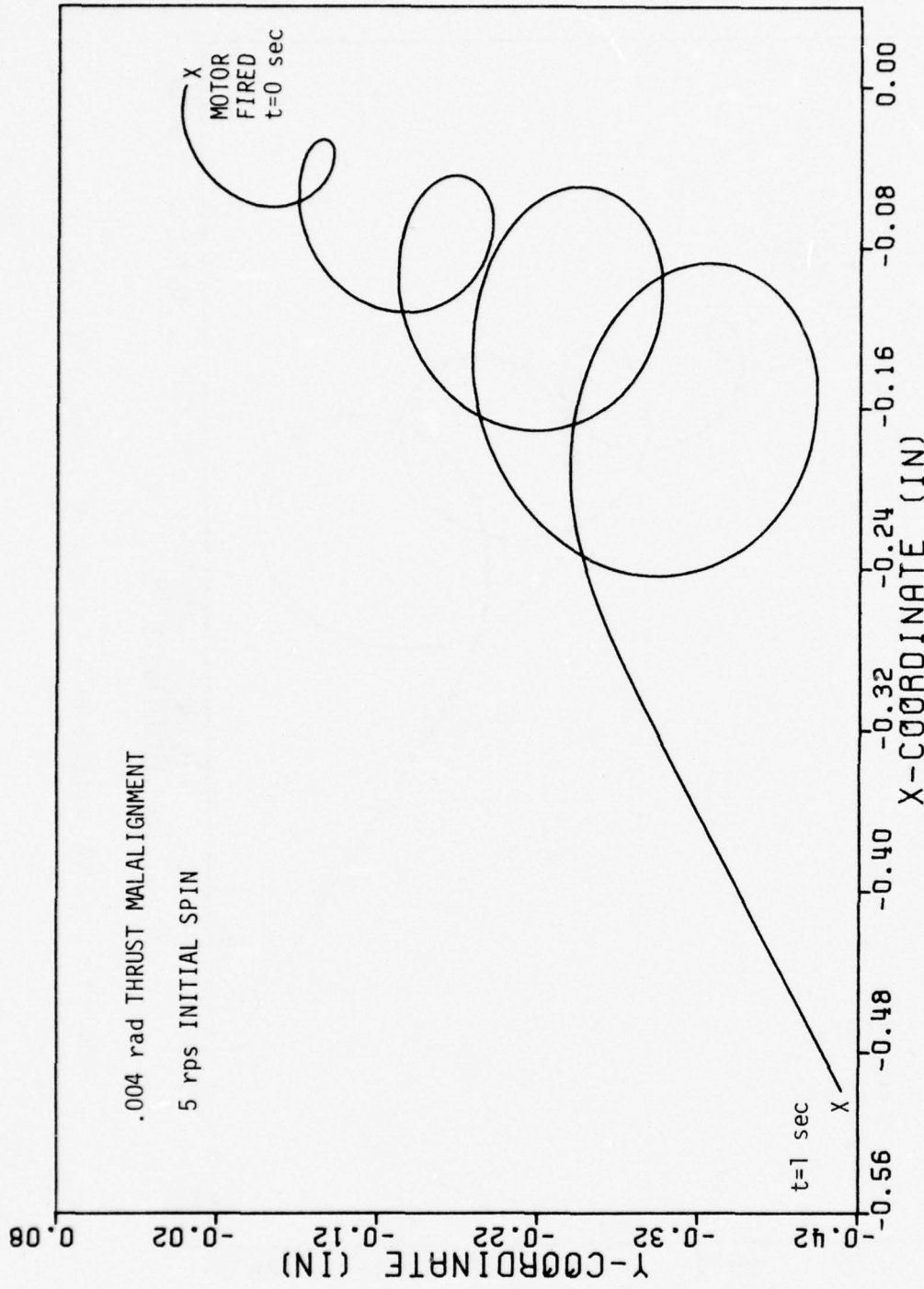


Figure 12. Nozzle Position as a Function of Time (5-.004)

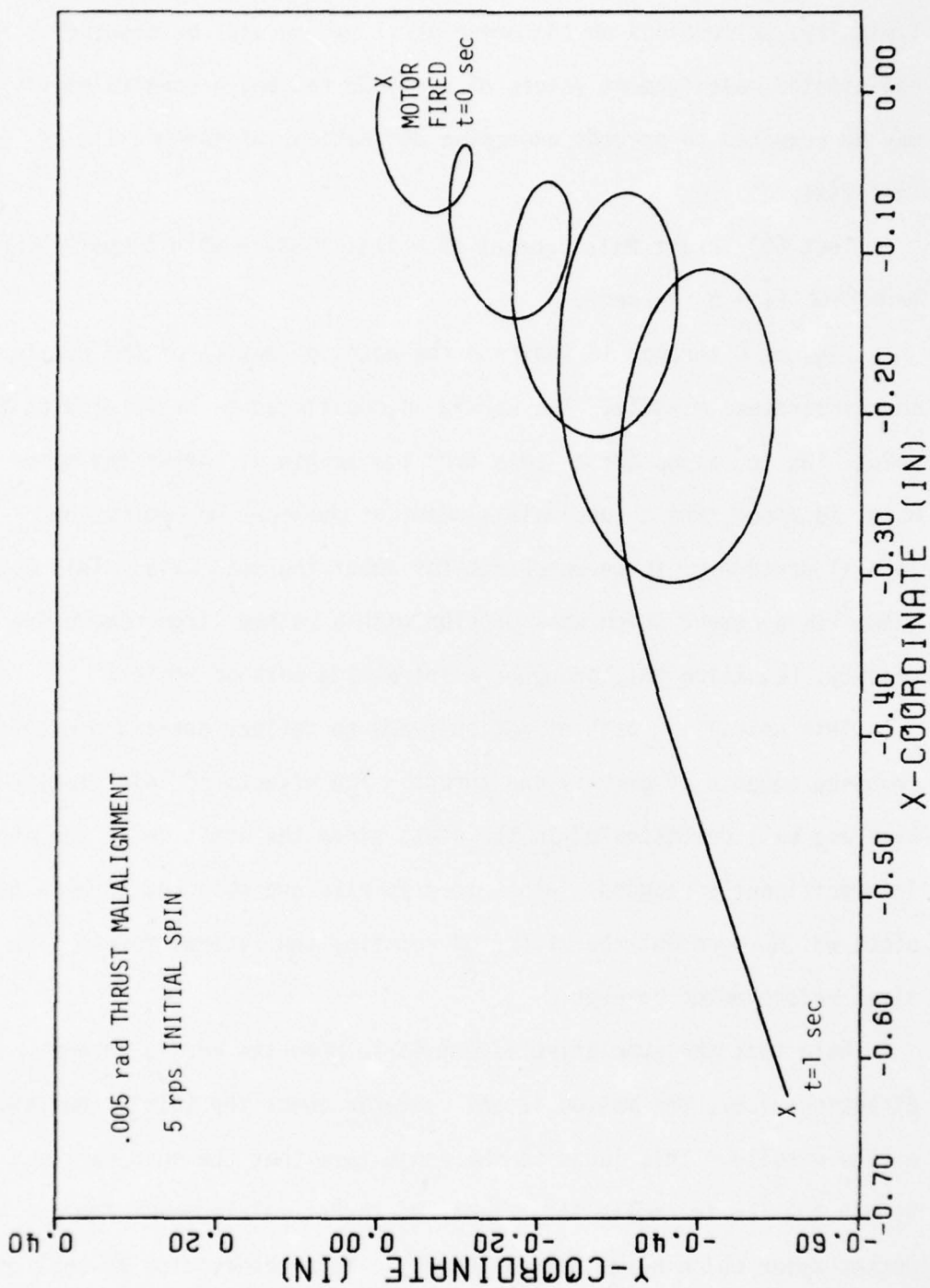


Figure 13. Nozzle Position as a Function of Time (5--.005)

Figure 6), indicates that large deflections of the missile will occur. Typically, deflections on the order of .1 radian will be observed. For anticipated malalignment values of $\alpha = .005$ radian, a constraint ring may be required to prevent excessive deflections of the missile in the test fixture.

Test (b) Thrust Malalignment of a Test Missile with 5 rps Initial Spin Rate ($\dot{\phi} = 5$ rev/sec).

Figures 9 through 13 indicate the paths of motion of the nozzle of the constrained missile. The nozzle is considered to be located at the point -135 in. along the z' axis from the origin 0. After the main motor is fired, the thrust malalignment of the missile results in a lateral perturbing force which rotates about the spin axis. This force generates a moment which when coupled with a rather large moment due to gravity, (equation 63), produces a spiralling path of motion.

This spiralling path of motion tends to deflect outward due to the combined moments of gravity and thrust. The effects of spin stabilization are well demonstrated in the plots since the nutation of the missile is significantly reduced. Also, four spirals are observed in each of the plots which represent the effect of rotating the lateral forces five times before motor burnout.

Note that the cumulative effect is to move the nozzle in one direction, i.e., the motion is not centered about the initial position of the missile. This leads to the conjecture that the spin rate may be far too low to negate the effects of thrust malalignment for a rocket motor which burns out so quickly. This observation is applicable to practically all the test investigated in this work. Of course, the extremely short burn time of .95 sec. should also be recalled.

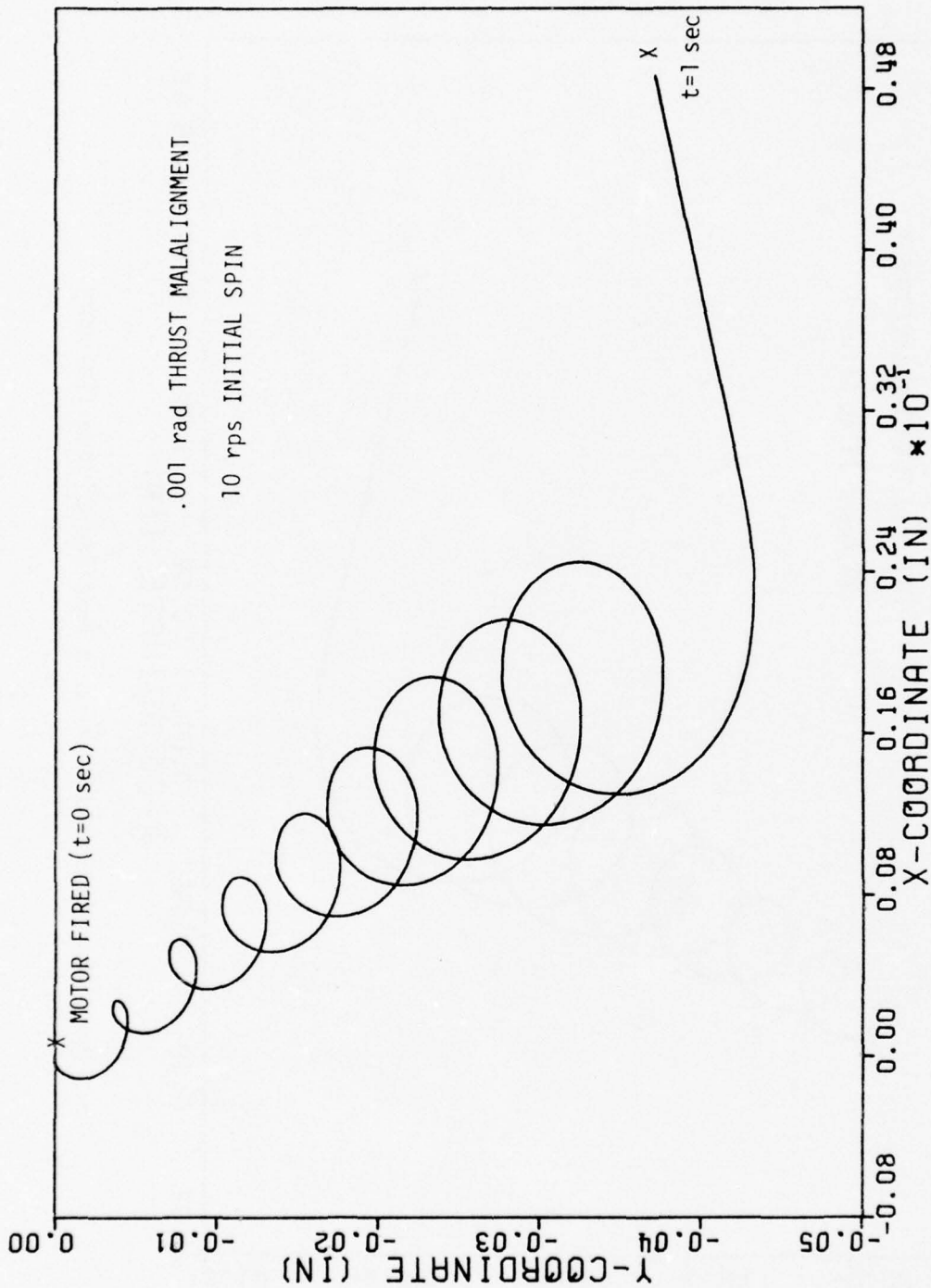


Figure 14. Nozzle Position as a Function of Time (10-.001)

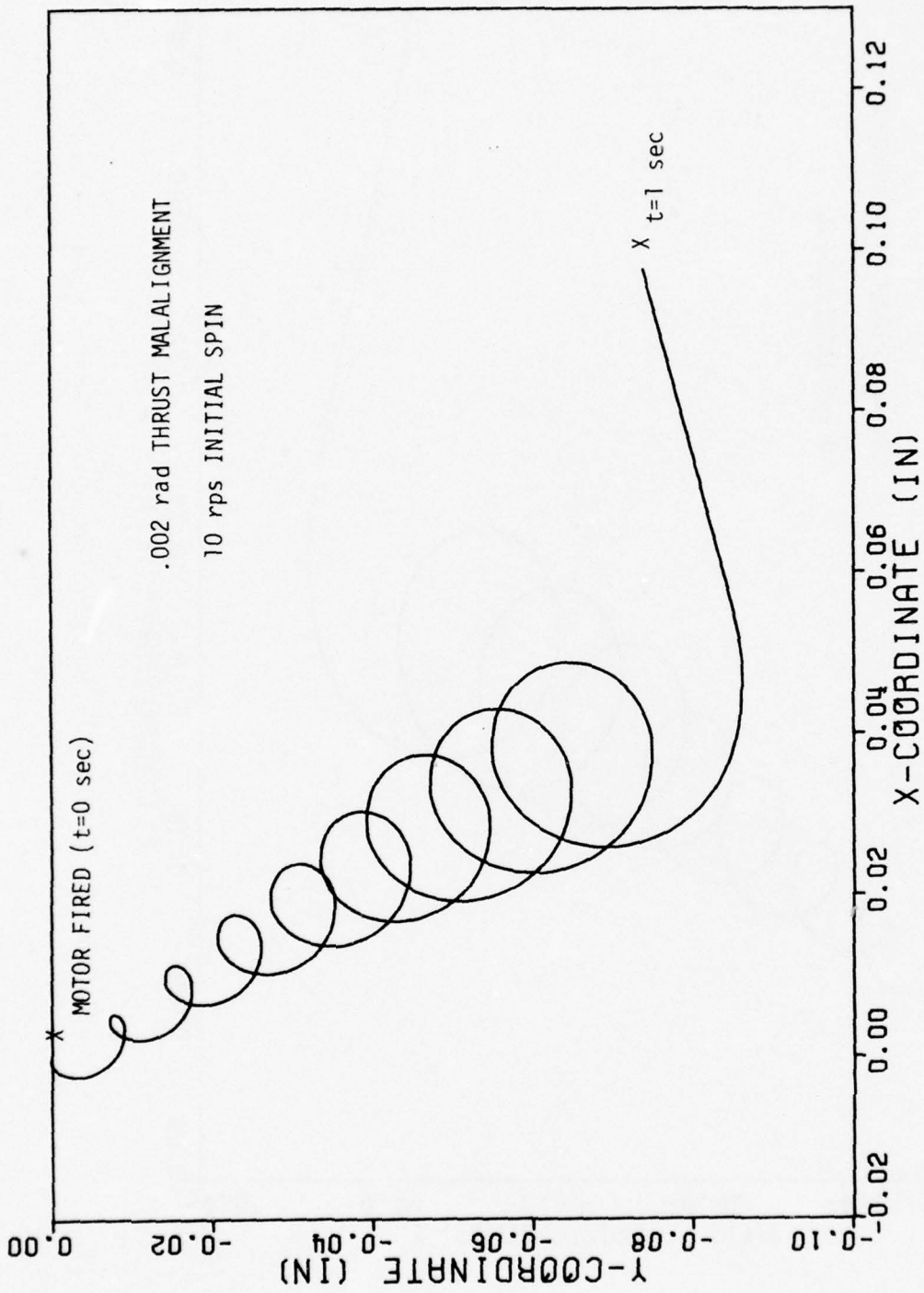


Figure 15. Nozzle Position as a Function of Time (10⁻³ sec)

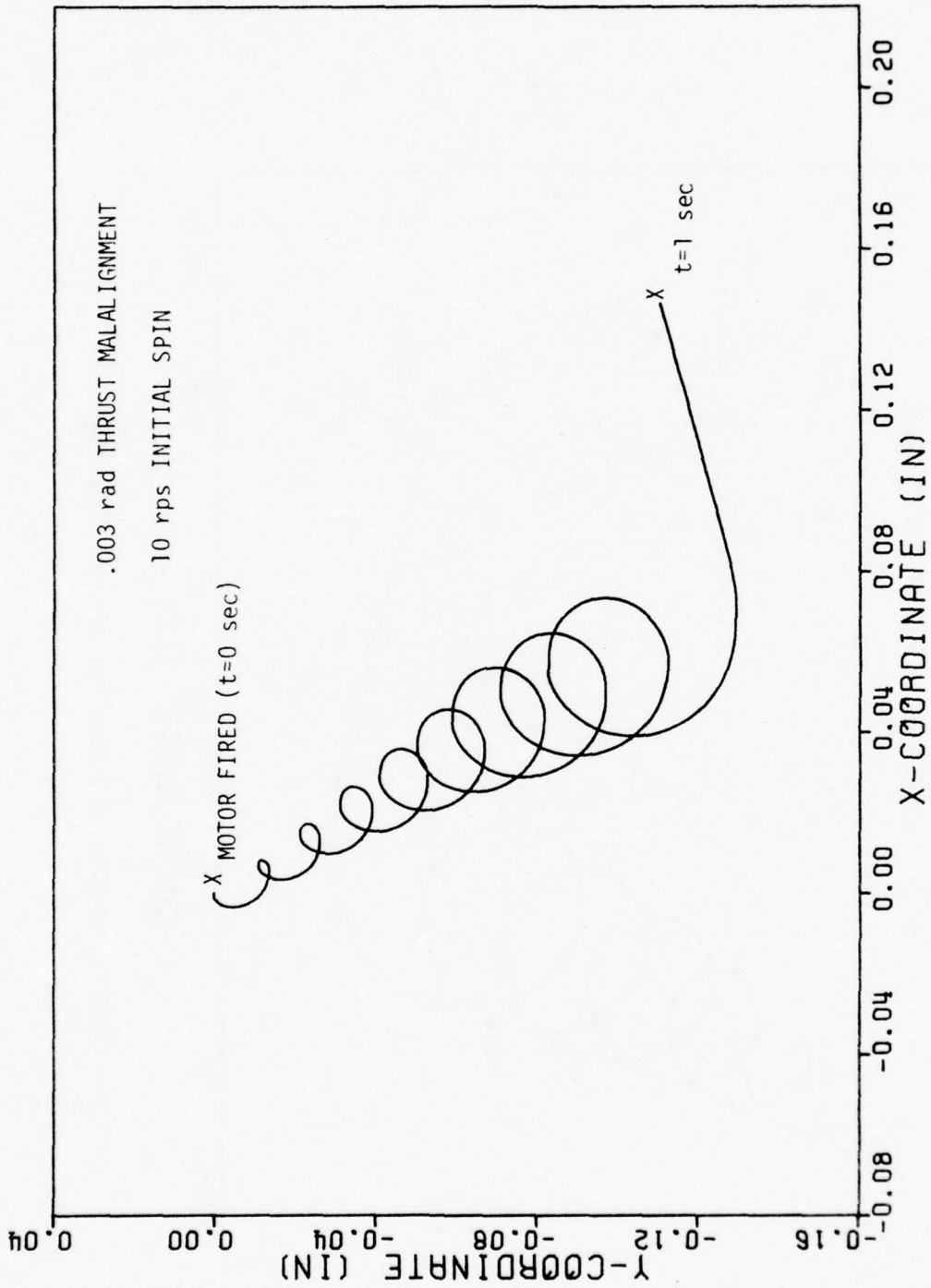


Figure 16. Nozzle Position as a Function of Time (10-.003)

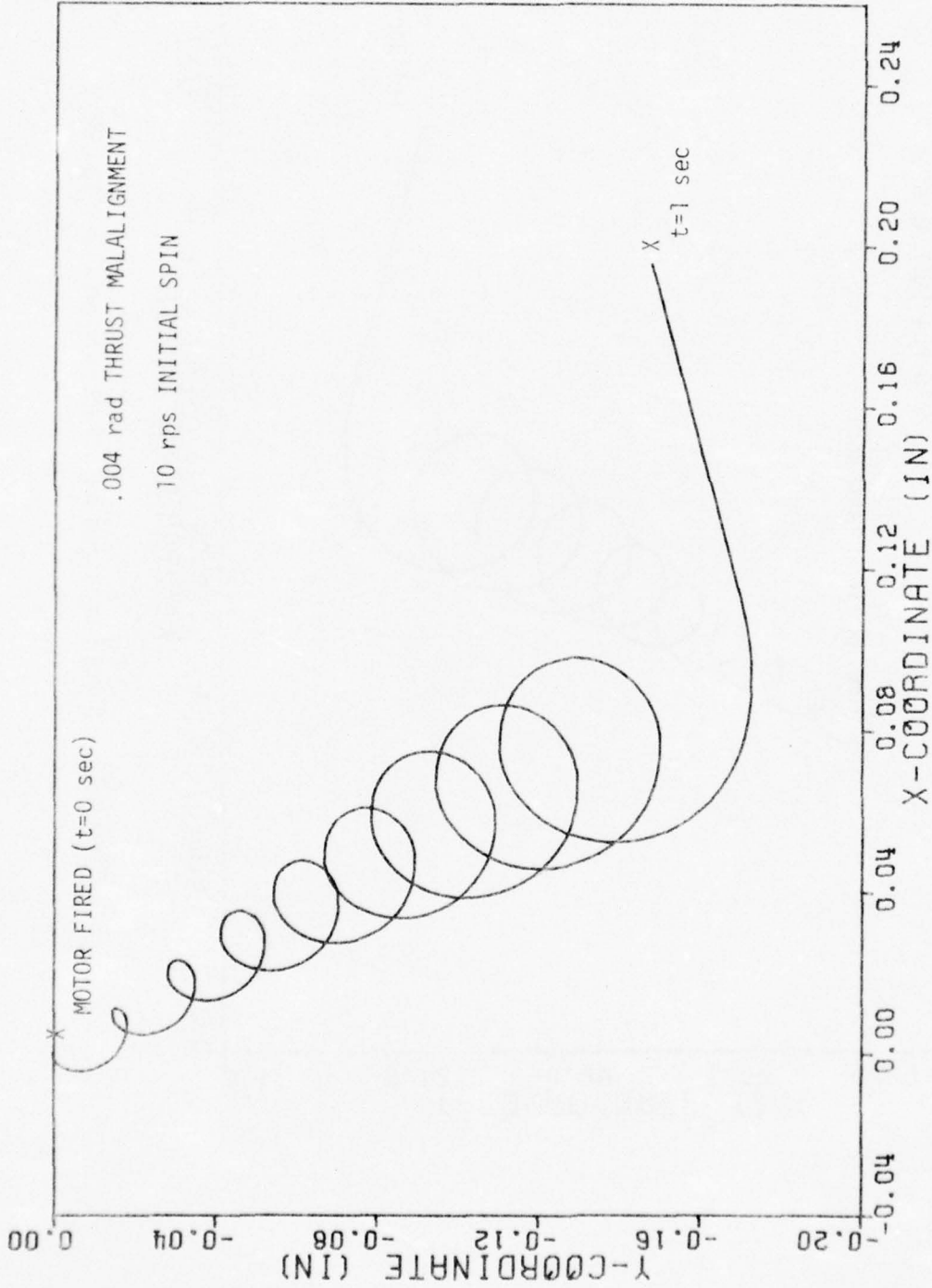


Figure 17. Nozzle Position as a Function of Time (10-.004)

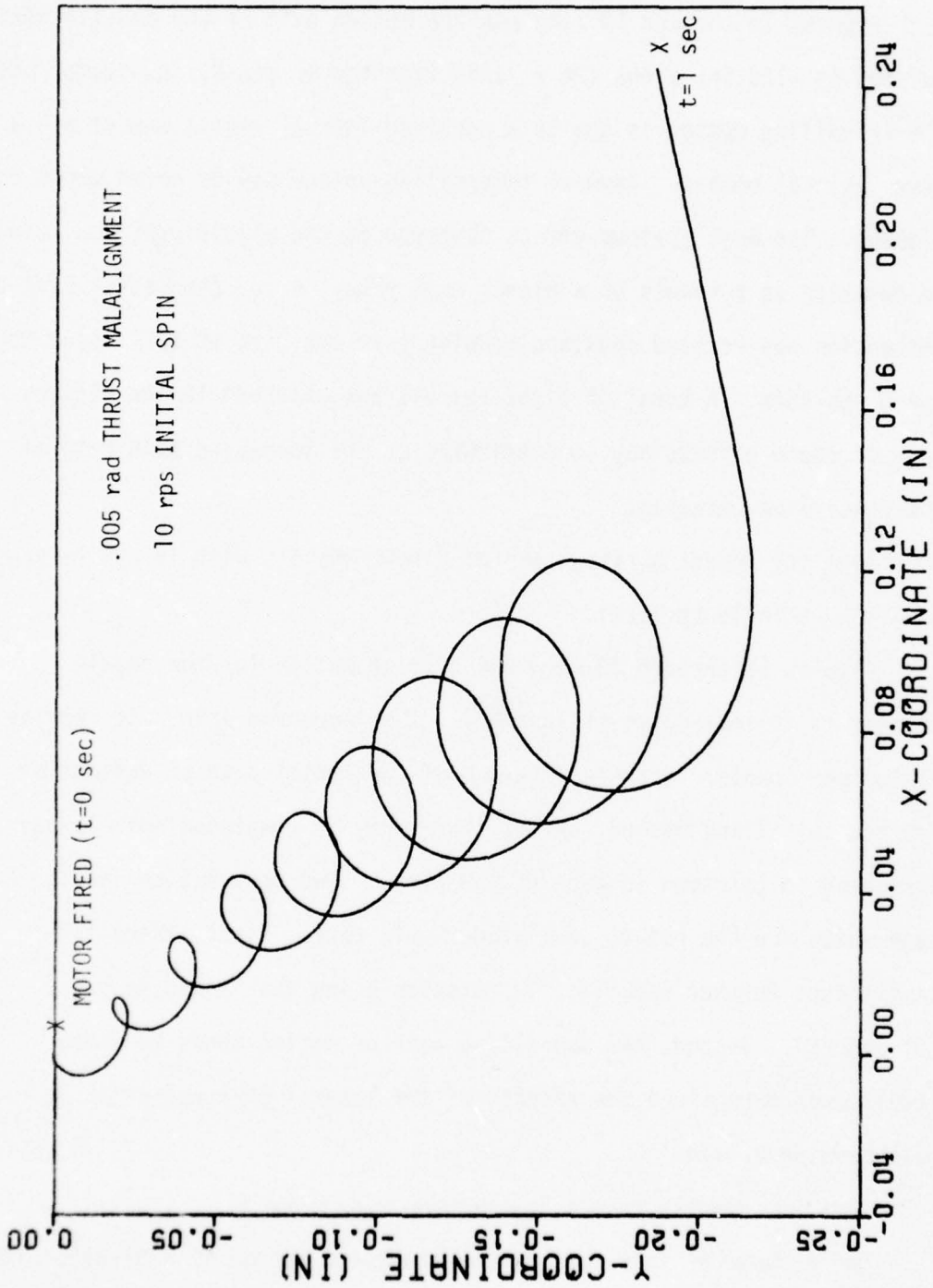


Figure 18. Nozzle Position as a Function of Time (10-.005)

Test (c) Thrust Malalignment of a Test Missile with 10 rps Initial Spin Rate ($\dot{\phi} = 10$ rev/sec).

Figures 14 through 18 simulate the motion path of the missile nozzle located at -135 in. along the z' axis from the origin 0. As stated before, the spiralling motion is due to a combined lateral thrust moment and a gravitational moment. Several interesting points may be noted about the figures. The most obvious effect observed is the significant reduction in nutation as a result of a higher spin rate. Also, the radial path of deflection has rotated counterclockwise from the path of deflection for the 5 rps case. A total of eight spirals are observed in the figures. Each of these effects may be attributed to the increased spin rate of the constrained missile.

Test (d) Thrust Malalignment of a Test Missile with 15 rps Initial Spin Rate ($\dot{\phi} = 15$ rev/sec).

Figures 19 through 23 show the path of motion for the nozzle located as in test cases (b) and (c). The increased spin rate results in further counterclockwise rotation of the radial path of deflection for the spiralling motion. Also, the number of completed spirals has increased to thirteen in each of the plots. Two observations may be made which are the result of a higher spin rate. First, there is a significant further reduction in nutation below that found in cases (b) and (c). Second, the spiralling path of motion tends to cross itself much more since the effects of the lateral perturbing forces have been decreased.

Test (e) Results from a Square Wave Thrust Impulse.

The purpose of this test was to study the motion of a missile with identical inertia and mass characteristics as in cases (a) through (d),

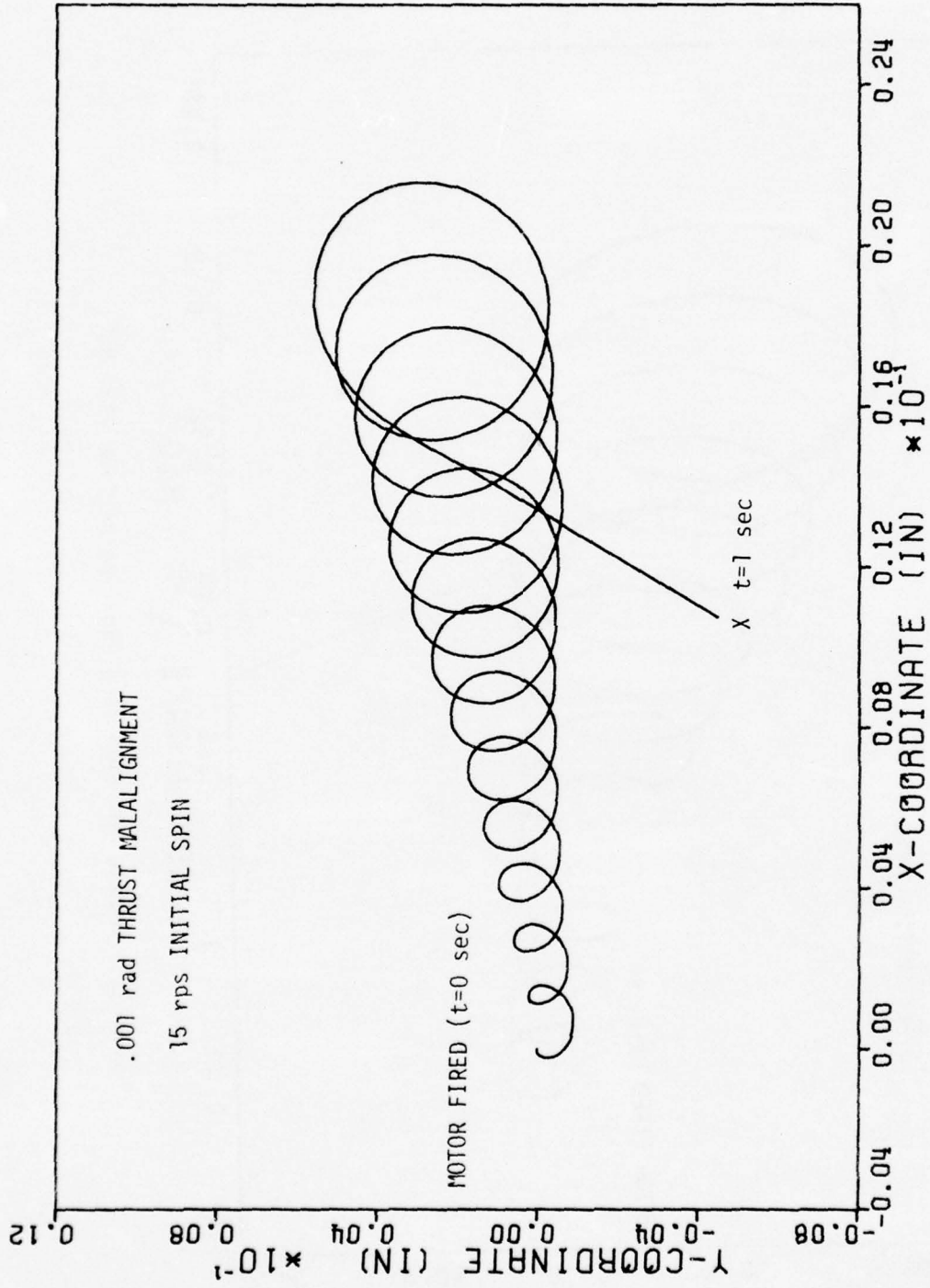


Figure 19. Nozzle Position as a Function of Time (15-.001)

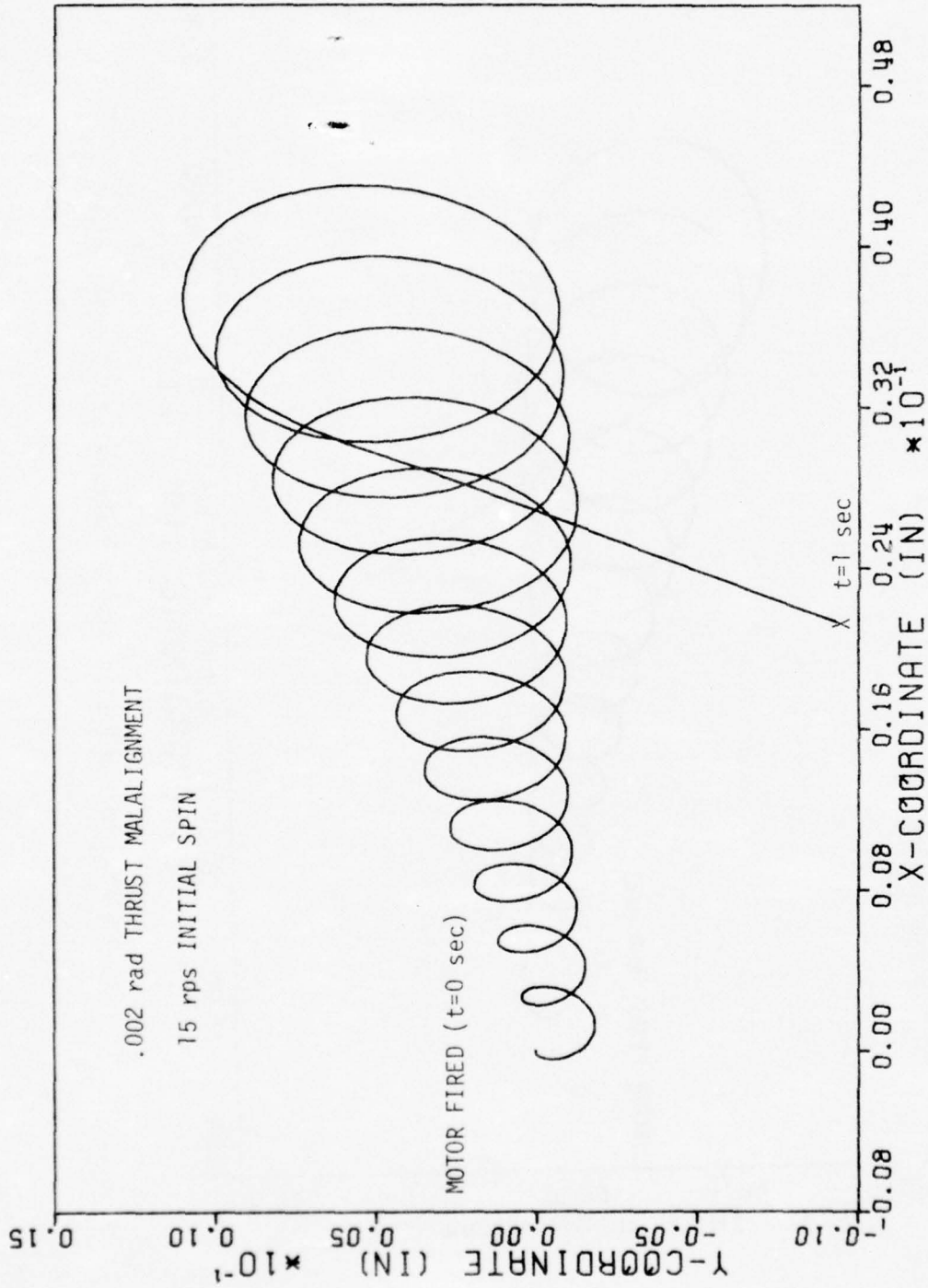


Figure 20. Nozzle Position as a Function of Time (15-.002)

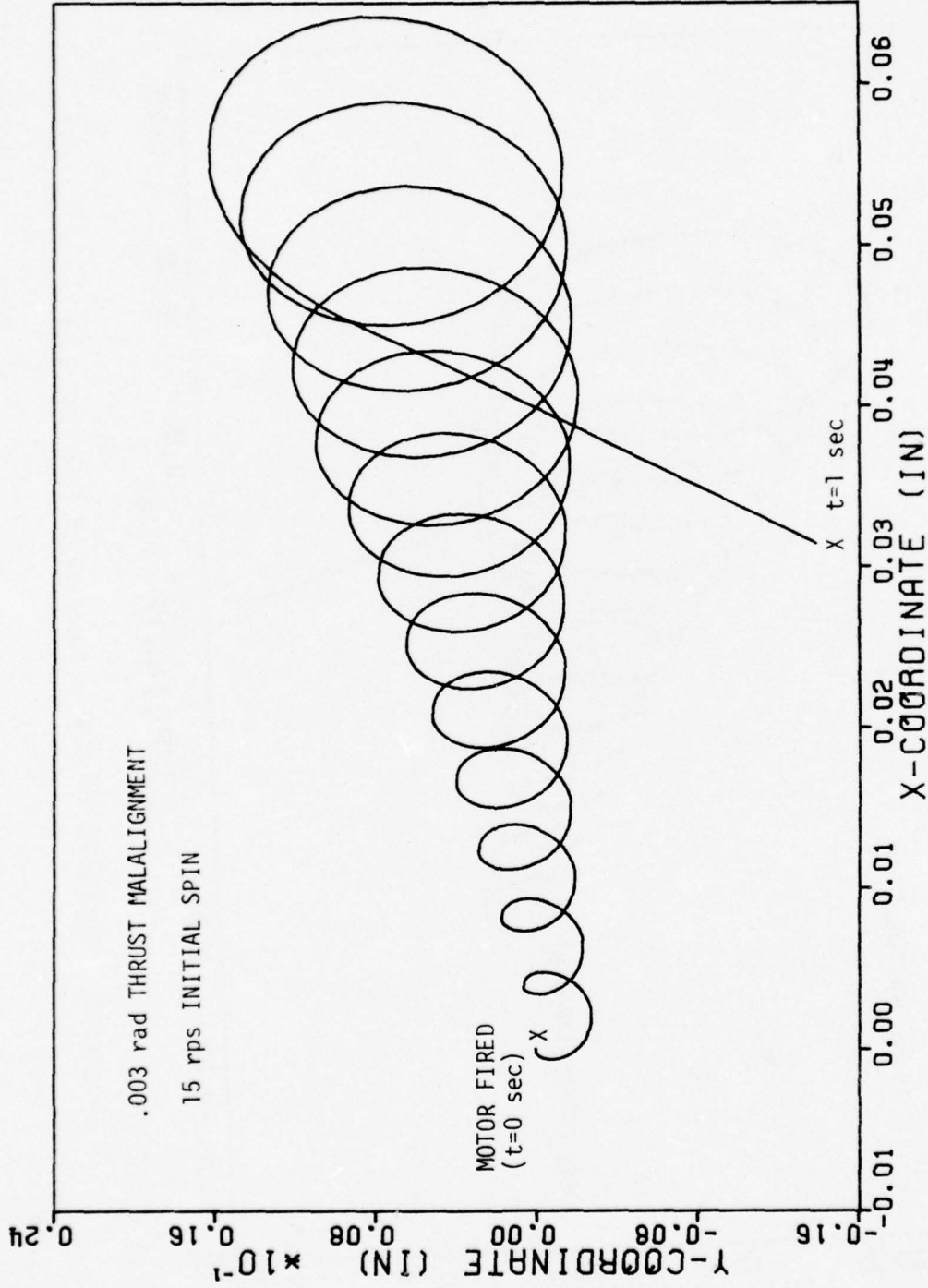


Figure 21. Nozzle Position as a Function of Time (15-.003)

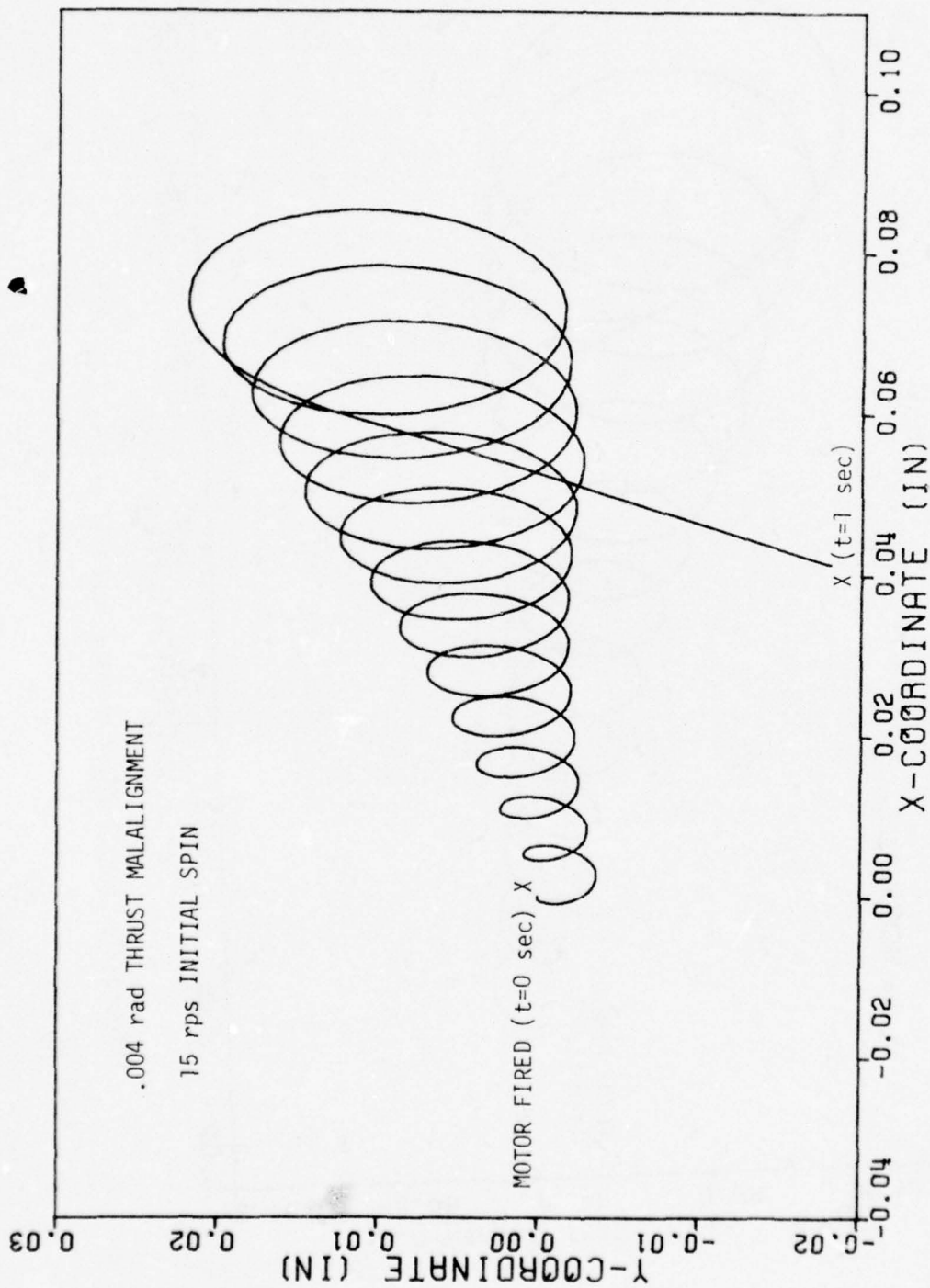


Figure 22. Nozzle Position as a Function of Time (15-.004)

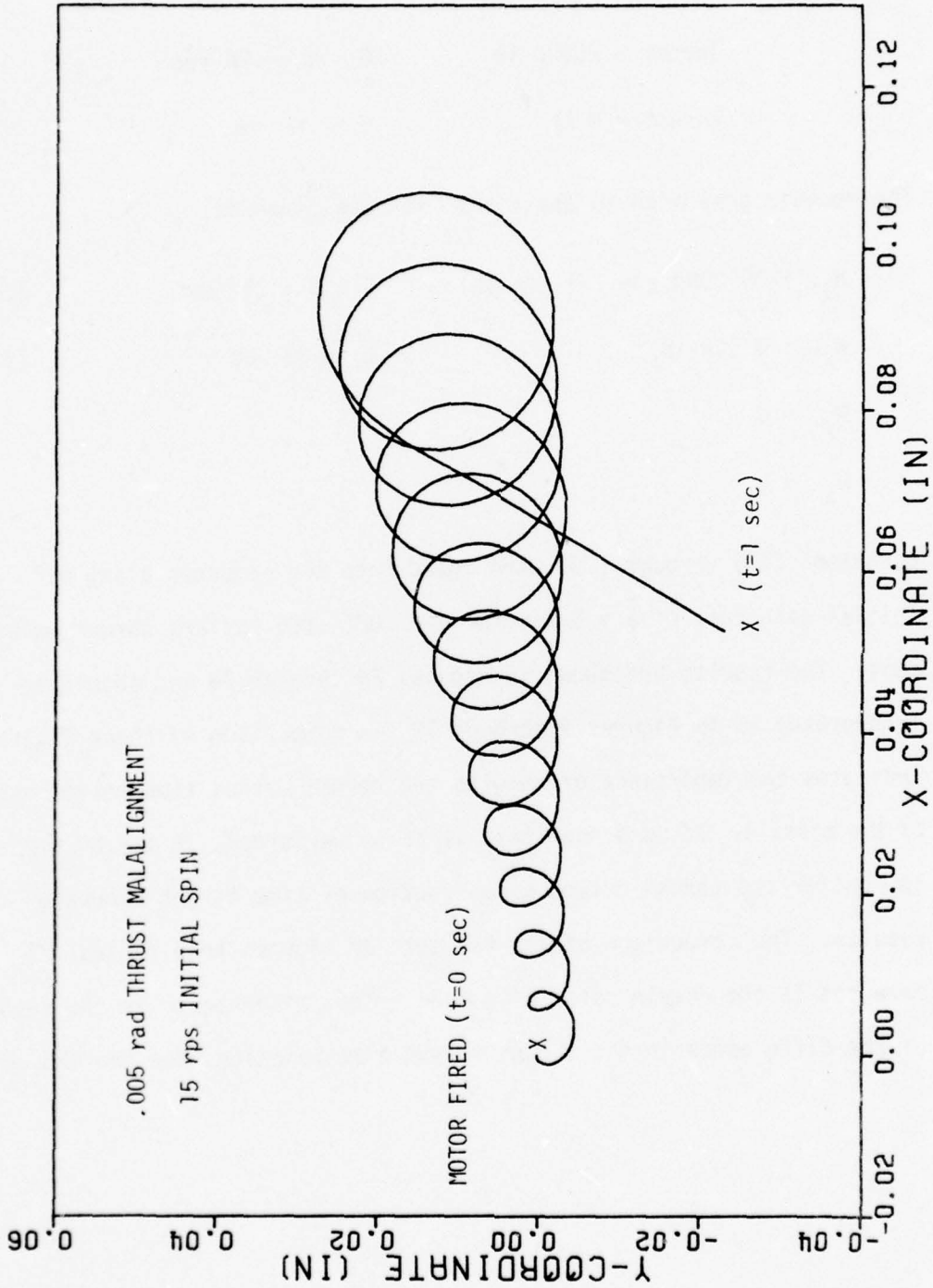


Figure 23. Nozzle Position as a Function of Time (15--005)

except that the thrust relation is a square wave. Consider a missile with a thrust output,

$$\begin{aligned} \text{Thrust} &= 26000 \text{ lb} & 0 \leq t \leq .90 \text{ sec} \\ \text{Thrust} &= 0 \text{ lb} & t > .90 \text{ sec} \end{aligned}$$

The moments generated in the $x'y'z'$ set are given as:

$$M_{x'} = 3510000 \sin(\alpha) \text{ (in-lb)} \quad 0 \leq t \leq .90 \text{ sec} \quad (69)$$

$$M_{x'} = 0 \text{ (in-lb)} \quad t > .90 \text{ sec} \quad (70)$$

$$M_{y'} = 0$$

$$M_{z'} = 0$$

Equations (63) through (70) were coded into the computer along with an initial spin rate of $\dot{\phi} = 5$ rps for $\alpha = .001-.005$ radians thrust malalignment. The results are shown in Figures 24 through 28 and should be interpreted as in Figures 9 through 13. A comparison of these figures indicates the importance of knowing the thrust versus time relationship of the missile. If an actual test is to be performed, it may be necessary to monitor the thrust output as a function of time to get accurate results. The comparison of the two sets of figures show radical differences in the nozzle paths of motion. This discrepancy is the result of the differences in the thrust versus time relations for the two cases.

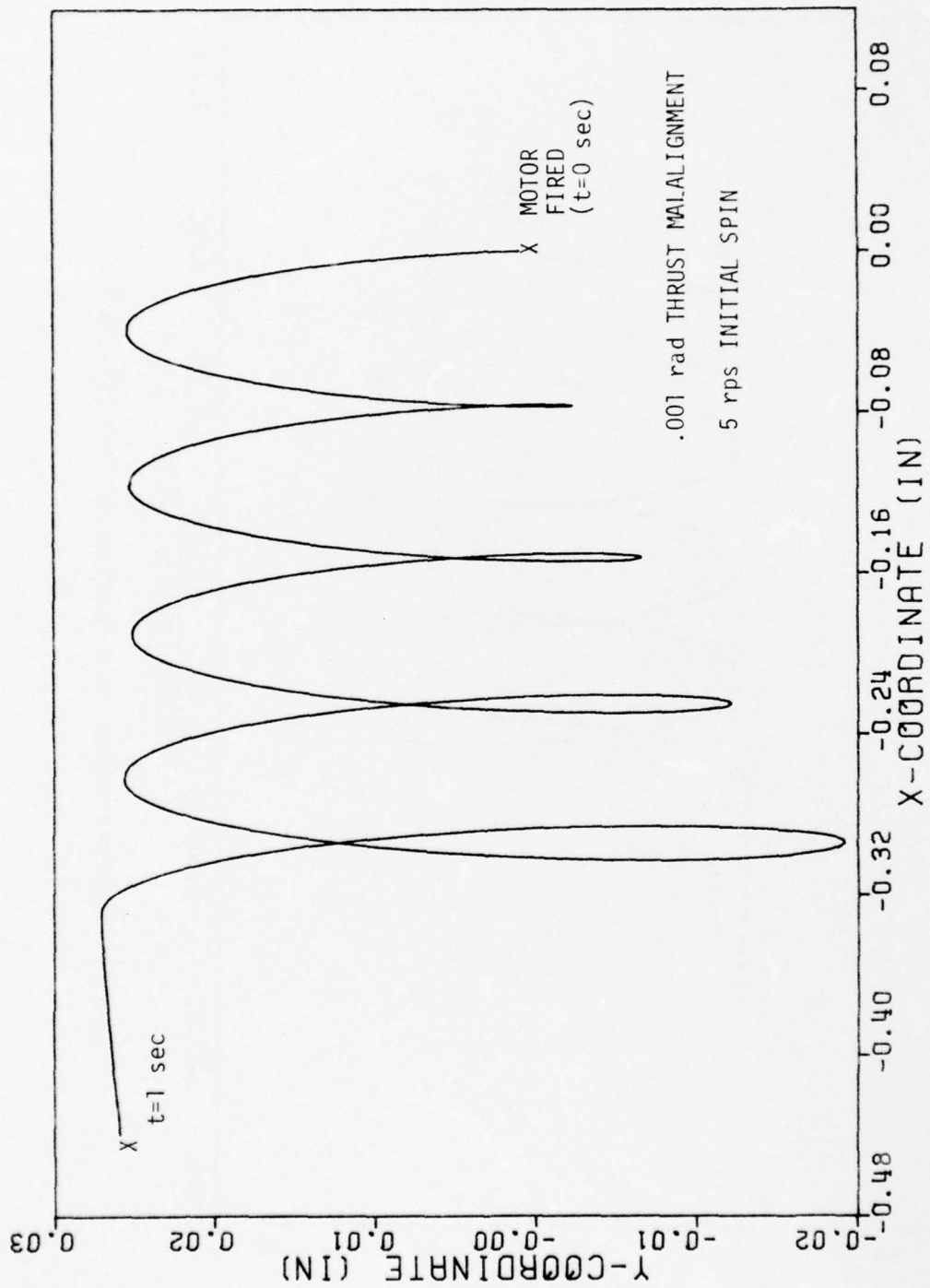


Figure 24. Nozzle Position as a Function of Time (S5--001)

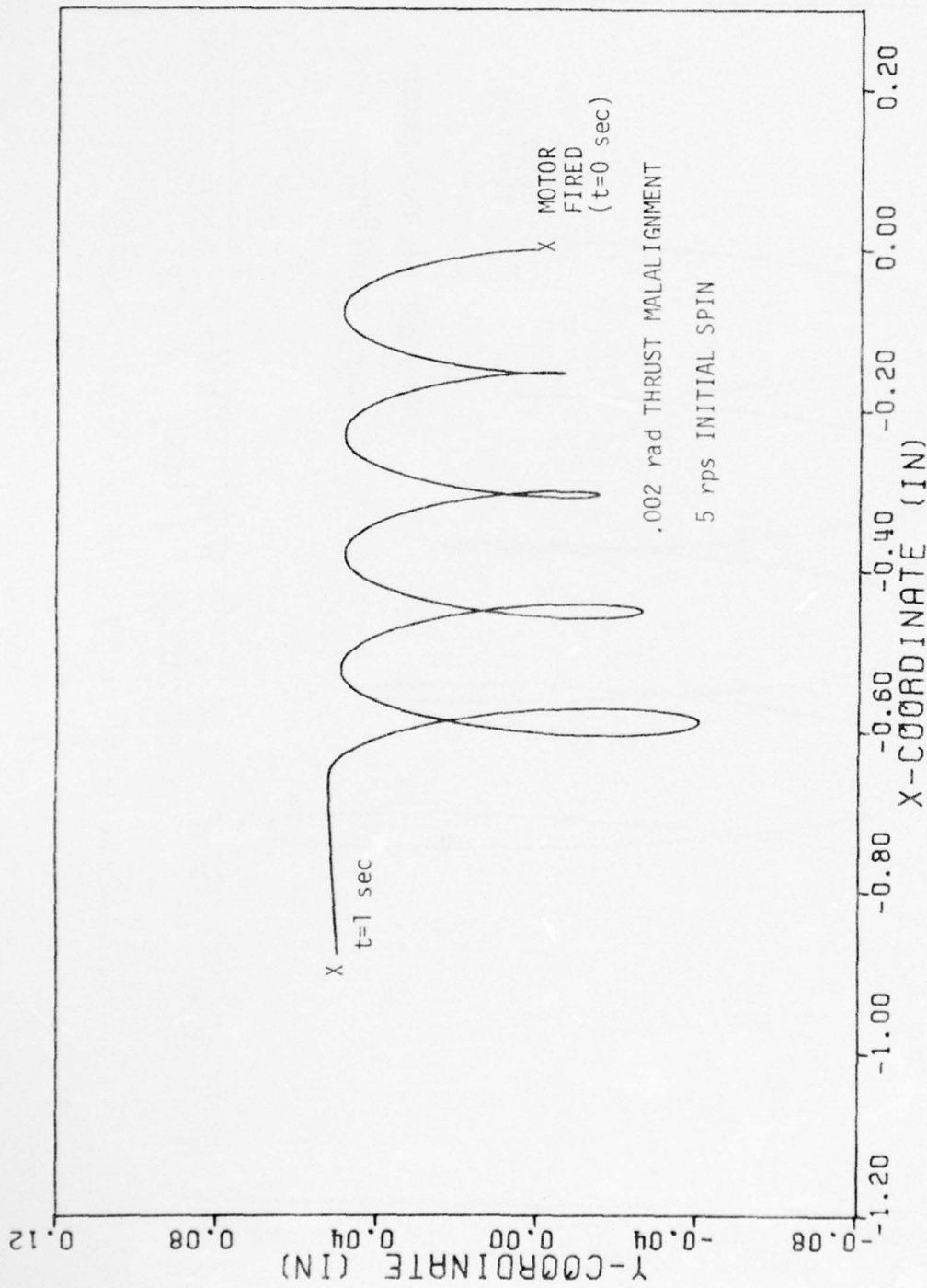


Figure 25. Nozzle Position as a Function of Time (S5-.002)

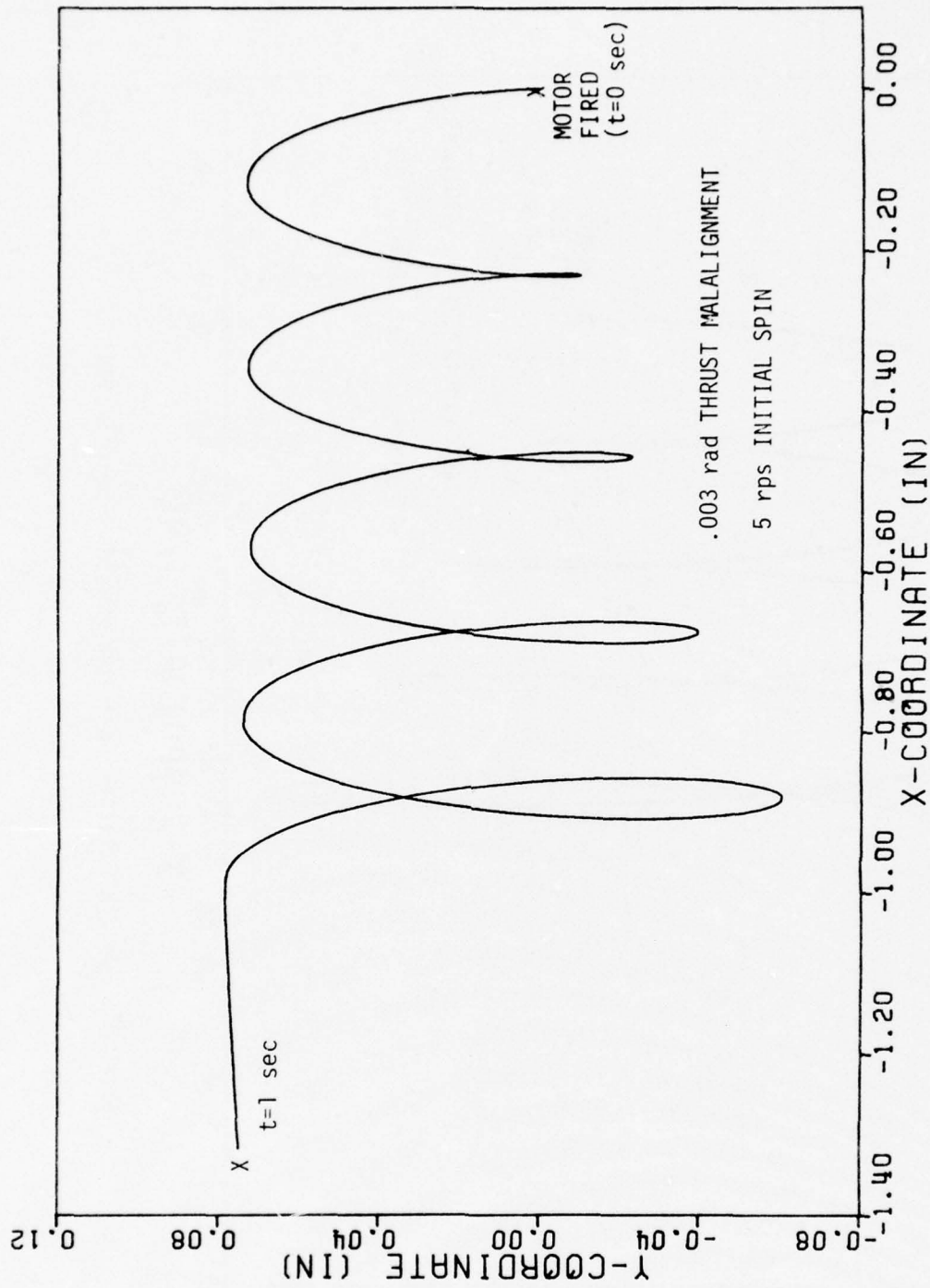


Figure 26. Nozzle Position as a Function of Time (S5--.003)

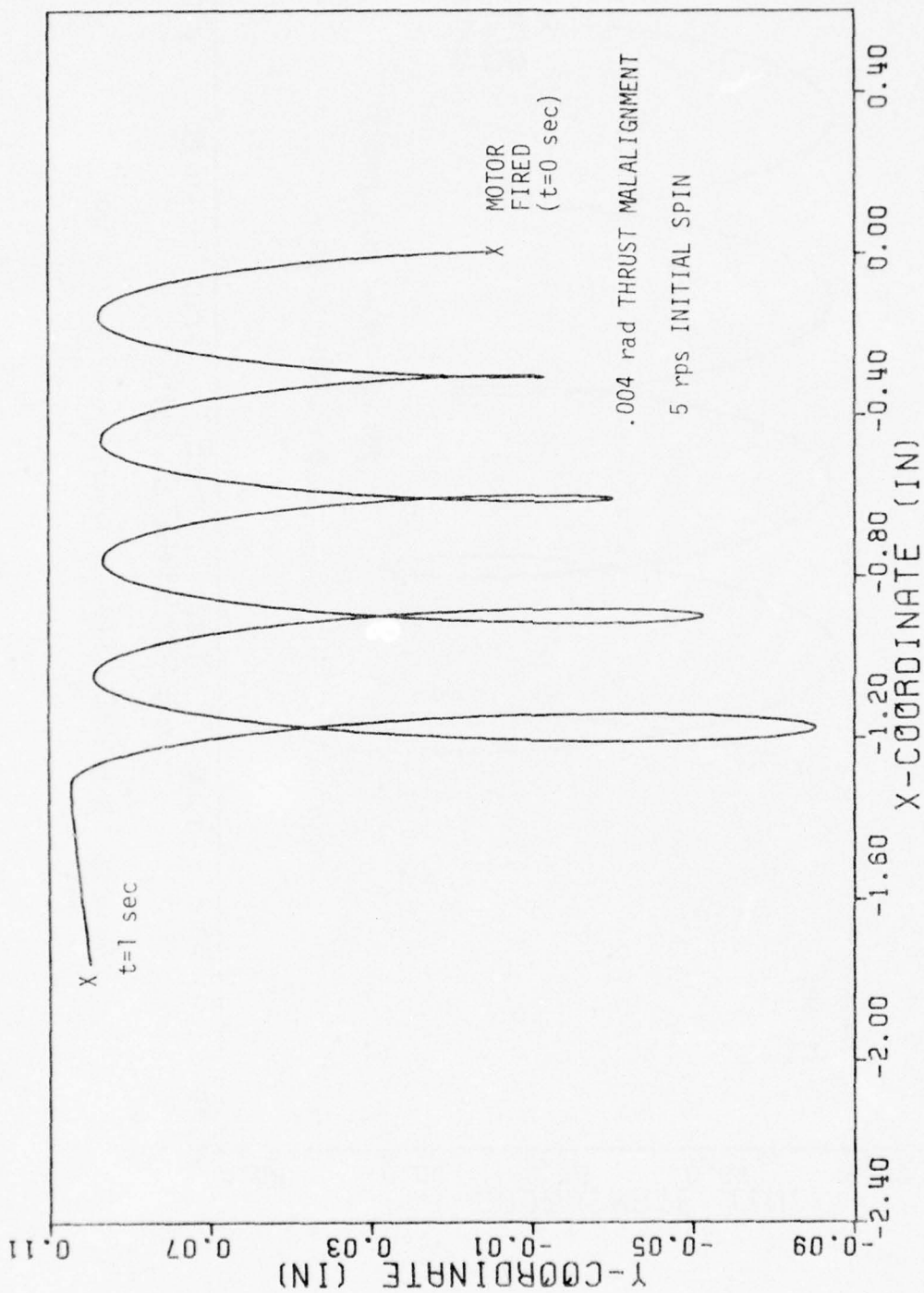


Figure 27. Nozzle Position as a Function of Time (S5-.004)

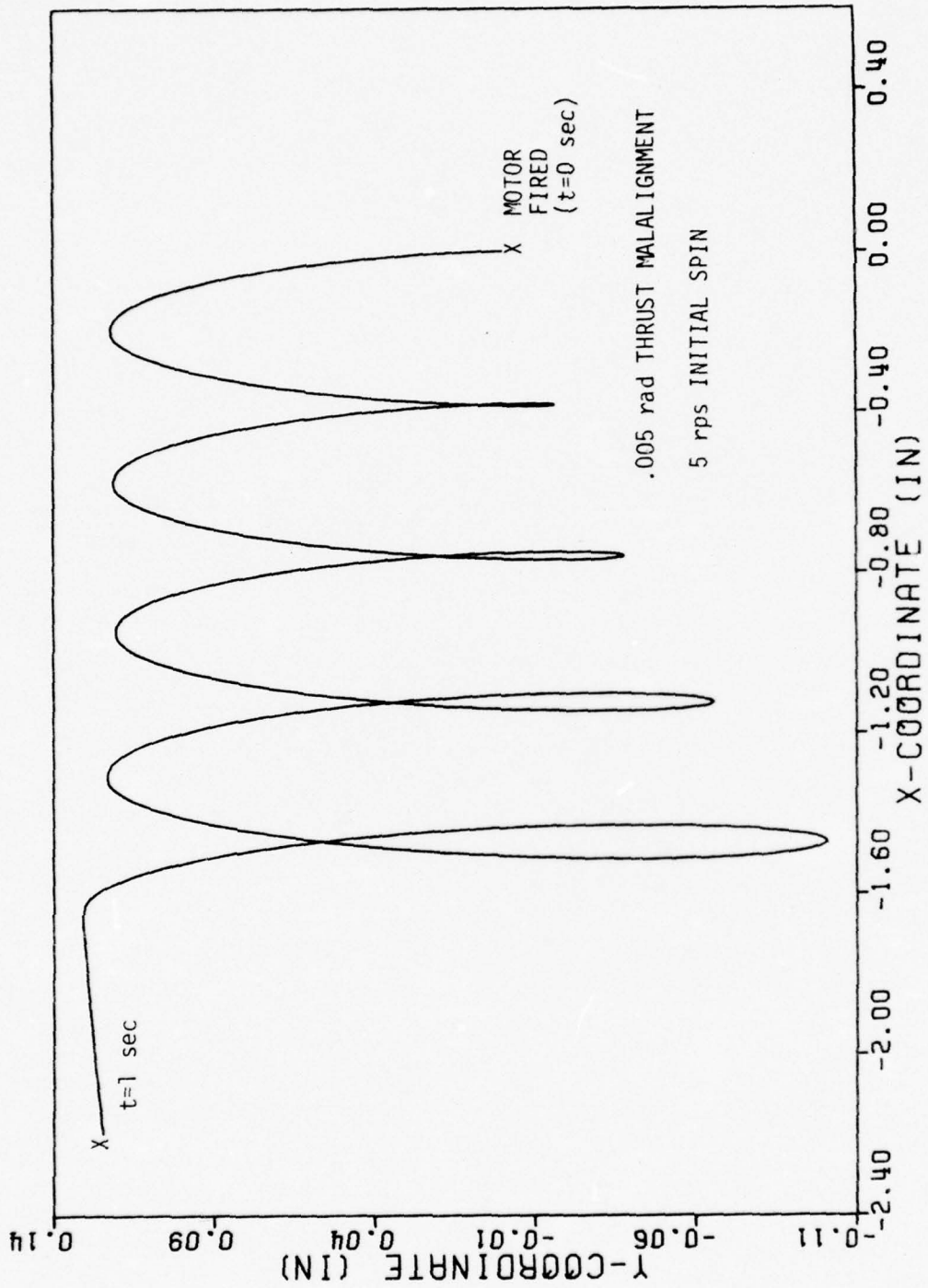


Figure 28. Nozzle Position as a Function of Time (S5-.005)

VI. CONCLUSIONS AND RECOMMENDATIONS

Results from the simulation studies for a test missile indicate that maximum nutation occurs when the initial spin rate is zero. If the maximum thrust malalignment is expected to exceed 5 mrad, then a constraint ring, (see Figure 1), should be considered for the test fixture. Results from the test cases also indicate that a knowledge of the thrust-time relationship is essential for making accurate predictions of the results of thrust malalignment. Also, the inertia and mass characteristics for the missile during the motor burning phase are required.

The most accurate way of predicting thrust malalignment appears to be the most simple. If the missile is not given an initial spin, maximum nutation will occur. Therefore, a very precise measurement of malalignment may be made. This study neglected all aerodynamic forces and frictional moments at the pivot joint of the test fixture. If the actual constraining device is built, consideration of these forces and moments may be included easily in the moment equations for the missile.

It should be recalled that the objective of this investigation was to determine the range of motion resulting from anticipated thrust malalignment anomalies affecting a typical rocket suspended in this unique ball and socket fashion. The results of the analysis show that:

- The motion ranges and motion rates are in the measurable regime.

- This scheme may be a viable experimental method for gathering performance data on real firings.

Further work needs to be done to examine questions of the effects of:

- Combined Unbalance and Thrust Malalignment
- Vibration and Buckling Phenomena
- Hardware Imperfections in the Mounting and Suspension Rig

APPENDIX I

Thrust Malalignment Computer Code

APPENDIX I

Thrust Malalignment Computer Code

The computer code for predicting the resultant motion of a missile for various degrees of thrust malalignment and initial conditions utilizes the following list of variables. The computer variable is listed first, followed by the mathematical equivalent.

$M1 = M_{x'}$ $M2 = M_{y'}$ $M3 = M_{z'}$	moments in the x'y'z' coordinate system
$M4 = M$	WR_{gz} component in the xyz coordinate system
$I1 = I$ $I2 = \dot{I}$	$I_{x'z'}$ inertia component and derivative (roll inertia)
$I3 = I'$ $I4 = \dot{I}'$	$I_{x'x'} = I_{y'y'}$ inertia component and derivative (Transverse Inertia)
$A1 = \psi$ $A2 = \dot{\psi}$ $A3 = \ddot{\psi}$	Euler angle precession components
J	number of ΔT intervals between successive printings of output
I	total number of output printings

A4 = θ		Euler angle nutation components
A5 = $\dot{\theta}$		
A6 = $\ddot{\theta}$		
A7 = ϕ		Euler angle spin components
A8 = $\dot{\phi}$		
A9 = $\ddot{\phi}$		
B1 = β		basic control variables (see equations (24) through (29))
B2 = μ		
B3 = ν		
B4 = λ		
B5 = ϵ		
B6 = ρ		
X = x		location of the missile nozzle in the XYZ coordinate system
Y = y		
R = R		-z location of the missile nozzle
A = α		thrust malalignment (radians)
T = ΔT		integration time interval
T1		total elapsed time
		Note: T1 = I*J*T

```

//ROCKET JOB (MED49,FORMS=6550),'70 SCHAEFFEL',CLASS=X
//STEPL EXEC FORTGCLG
//FORT.SYSIN DD *
C-----THRUST MALALIGNMENT COMPUTER CODE-----
REAL I1,I2,I3,I4,M1,M2,M3,M4
DO 5 K=1,5,1
A=.001*FLOAT(K)
C-----ZERO THE DATA BASE-----
A1=0.
A2=0.
A3=0.
A4=0.
A5=0.
A6=0.
A7=0.
A8=0.
A9=0.
E1=0.
E2=0.
E3=0.
E4=0.
E5=0.
E6=0.
I1=0.
I2=0.
I3=0.
I4=0.
M1=0.
M2=0.
M3=0.
M4=0.
I=0.
I1=0.
C-----SET THE INITIAL CONSTRAINTS-----
I=500
J=20
T=.0001
C-----END OF INITIAL CONSTRAINTS-----
DO 4 L=1,I,1
DO 2 M=1,J,1
C-----SET THE SPATIAL CONSTRAINTS-----
IF (T1.LE..95) I1=-14.614*T1+43.155
IF (T1.LE..95) I3=-22428.59*T1+39196.92
IF (T1.LE..95) M4=-1252.619*T1*T1+8966.3*T1-15391.2
M1=0.
IF (T1.LT..95) M1=(-7.02E+7*T1+6.669E+7)*SIN((19.-20.*T1)*A)
IF (T1.LT..90) M1=3510000.*SIN(A)
IF (T1.LT..65) M1=(2475000.*T1+1890000.)*SIN((1.7051*T1+.5385)*A)
IF (T1.LT..05) M1=4.05E+7*T1*SIN(11.538*T1*A)
C-----END OF SPATIAL CONSTRAINTS-----
P1=COS(A4)
P2=SIN(A4)
P3=A2*P1
P4=A2*P2
P5=COS(A7)
P6=SIN(A7)
IF (P2.EQ.0.) GOTO 1
A3=(M1*P6+M2*P5-I4*P4+(I1*(A8+P3)-2.*I3*P3)*A5)/(I3*P2)
1 A6=(M1*P5-M2*P6+M4*P2-I4*A5+(I3*P3-I1*(A8+P3))*P4)/I3
A9=(M3-I2*(A8+P3)-I1*(A3*P1-A5*P4))/I1

```

```
A1=A2*T+A1
A2=A3*T+A2
A4=A5*T+A4
A5=A6*T+A5
A7=A8*T+A7
A8=A9*T+A8
2  T1=T1+T
   WRITE(10,3) T1,A4,A5,A6
3  FORMAT(4E15.4)
4  CONTINUE
5  CONTINUE
   STOP
   END
//GC.FT10F001 DD DSN=MED48.BINGO,DISP=(NEW,CATLG),
// LABEL=(1,SL),UNIT=TAPE,DCB=(RECFM=FBS,LRECL=60,BLKSIZE=13020)
//GC.SYSIN DD *
//STEP2 EXEC TAPEFILE
//SYSIN DD *
FILE DSNAME=MED48.BINGO
```

JCB

CPL TIME=

0.12 SEC

```

//ROCKET JOB (MED48,FORMS=6550),*70 SCHAEFFEL*,CLASS=X
//MSGLEVEL=1
//STEPA EXEC 7AP
//SYSIN DD *
      DSNAME=MED48.DATER
//STEPB EXEC PLOTCLG,PARM.FORT='LIST,MAP',REGION=170K
//FORT.SYSIN DD *
C-----TRUST MALALIGNMENT PLOTTER CODE
      DIMENSION A(5,500),B(5,500),C(5,500),D(5,500)
      REWIND IC
      DC 3 I=1,5,1
      DC 2 J=1,500,1
      READ(10,1) A(I,J),B(I,J),C(I,J),D(I,J)
1     FORMAT(4E15.4)
2     CONTINUE
3     CONTINUE
      CALL GSIZE(50.0,11.0,1121)
      CALL SPPLLOT(A,' ',1,B,' ',1,' ',1,7.5,5.0,C,5,500,1121)
      CALL PLOT(8.0,-2.5,-3)
      CALL SPPLLOT(A,' ',1,C,' ',1,' ',1,7.5,5.0,D,5,500,1121)
      CALL PLOT(8.0,-2.5,-3)
      CALL SPPLLOT(A,' ',1,D,' ',1,' ',1,7.5,5.0,0,5,500,1121)
      CALL PLOT(0.0,0.0,999)
      STOP
      END
      SUBROUTINE SPPLLOT(X,XHDR,KX,Y,YHDR,KY,FHDR,KF,
1ALENX,ALENY,LINTYP,NROW,NCOL,JPEN)

```

```

C
C
C   SPPLLOT IS A SUBROUTINE THAT WILL PLOT NROW NUMBER OF
C   LINES PER GRAPH. (WRITTEN BY GERRY A. LINDHOLM)
C
C   THE ARGUMENTS OF THE LIST ARE:
C       X   NAME OF THE ARRAY CONTAINING THE ABSCISSA OR X
C           VALUES.
C       XHDR AND KX DESCRIBE THE DESIRED LEGEND FOR THE
C       X-AXIS.
C       XHDR IS THE LITERAL EXPRESSION OF THE LEGEND TO BE
C       PRINTED.
C       KX IS THE INTEGER NUMBER OF CHARACTERS IN XHDR (LIMIT
C       20 CHARACTERS).
C       Y   NAME OF THE ARRAY CONTAINING THE ORDINATE OR Y
C           VALUES.
C       YHDR AND KY DESCRIBE THE DESIRED LEGEND FOR THE
C       Y-AXIS.
C       YHDR IS THE LITERAL EXPRESSION OF THE LEGEND TO BE
C       PRINTED.
C       KY IS THE INTEGER NUMBER OF CHARACTERS IN YHDR (LIMIT
C       20 CHARACTERS).
C       FHDR AND KF DESCRIBE THE DESIRED LEGEND FOR THE GRAPH HEADING,
C       LIMIT 100 CHARACTERS.
C       FHDR IS THE LITERAL EXPRESSION OF THE HEADING TO BE PRINTED.
C       KF IS THE INTEGER NUMBER OF CHARACTERS IN THE HEADING.
C       ALENX IS THE DESIRED LENGTH OF THE X-AXIS IN INCHES NOT TO
C       EXCEED 8.5 INCHES.
C       ALENY IS THE DESIRED LENGTH OF THE Y-AXIS IN INCHES NOT
C       TO EXCEED 8.5 INCHES.
C       LINTYP DETERMINES THE TYPE OF LINE YOU GET.
C       IF LINTYP GREATER THAN 0, YOU GET A STRAIGHT LINE
C       CONNECTING A SYMBOL PLOT DOWN AT EVERY LINTYP*TH

```

C POINT.
 C THUS, IF LINTYP WERE EQUAL TO 2, YOU WOULD GET A
 C LINE CONNECTING EVERY SECOND POINT.
 C IF LINTYP WERE EQUAL TO 0, YOU WILL GET A LINE
 C ONLY.
 C IF LINTYP LESS THAN 0, YOU WOULD GET A SYMBOL
 C EVERY LINTYPTF POINT.
 C NROW IS AN INTEGER NUMBER THAT TELLS THE NUMBER OF
 C LINES DRAWN ON THE GRAPH.
 C NCOL IS AN INTEGER NUMBER FOR THE NUMBER OF DATA POINTS
 C ON EACH LINE.
 C IPEN IS THE TYPE OF PEN USED TO MAKE THE GRAPH,
 C I.E. BALL POINT PEN, BLACK RAPIDOGRAPH PEN, ETC. (REFER
 C TO THE PLOTTER MANUAL SUPPLIED BY THE COMPUTER CENTER UNDER
 C C SIZE).
 C

```

DIMENSION X(NROW,NCOL), Y(NROW,NCOL), XHDR(20),
1YHDR(20), FHDR(100)
CALL SYMBOL(2.5,1.0,.15,FHDR,C.0,KF)
CALL PLOT(2.5,2.5+ALENY,3)
CALL PLOT(2.5+ALENX,2.5+ALENY,2)
CALL PLOT(2.5+ALENX,2.5,2)
CALL PLOT(2.5,2.5,-3)
CALL SCALE2(X,ALENX,NROW,NCOL,FRX,DLX)
CALL SCALE2(Y,ALENY,NROW,NCOL,FRY,DLY)
CALL AXIS(C.0,C.0,XHDR,-KX,ALENX,C.0,FRX,DLX)
CALL AXIS(C.0,C.0,YHDR,KY,ALENY,90.0,FRY,DLY)
DO 32 J=1,NROW
IF(J.NE. 1) CALL PLOT(C.0,C.0,3)
INTEQ=J
IPEN = 3
ICCDF = -1
NT = IABS(LINTYP)
IF (LINTYP)7,6,7
6 NT=1
7 NF=1
NA = NT
KK=1
IF (LINTYP) 11,12,13
11 IPENA = 3
ICCDF = -1
LSW = 1
GO TO 15
12 NA=NCOL
13 IPENA = 2
ICCDF = -2
LSW=0
15 DO 30 I=1,NCOL
XN=(X(J,I)-FRX)/DLX
YN=(Y(J,I)-FRY)/DLY
IF (NA-NT) 20,21,22
20 IF (LSW) 23,22,23
21 CALL SYMBOL (XN,YN,C.08,INTEQ,C.0,ICCDF)
NA = I
GO TO 25
22 CALL PLOT (XN,YN,IPEN)
23 NA = NA + 1
25 NF = NF+KK
  
```

```

30 IPEN = IPENA
31 CONTINUE
32 CONTINUE
RETURN
END

```

```

C      SUBROUTINE SCALE2(ARRAY,AXLEN,NROW,NCOL,FIRST,DEL)
C      ARRAY      NAME OF ARRAY CONTAINING VALUES TO BE
C                  SCALED.
C      AXLEN      LENGTH IN INCHES OVER WHICH ARRAY IS TO
C                  BE SCALED.
C      NPTS       NUMBER OF POINTS TO BE SCALED.
C      INC        INCREMENT OF LOCATION OF SUCCESSIVE
C                  POINTS.

```

```

DIMENSION ARRAY(NROW,NCOL),SAVE(7)
SAVE(1)=1.0
SAVE(2)=2.0
SAVE(3)=4.0
SAVE(4)=5.0
SAVE(5)=8.0
SAVE(6)=10.0
SAVE(7)=20.0
FAD=0.01
INC=1
NPTS=NCOL
K=IABS(INC)
N=NPTS*K
Y1=1.0E60
YF=-1.0E-60
DO 26 JJ=1,NROW
YC=ARRAY(JJ,1)
YN=YC
DO 26 I=1,N,K
YS=ARRAY(JJ,I)
IF (YC-YS) 22,22,21
21 YC=YS
CC TO 25
22 IF (YS-YN) 25,25,24
24 YN=YS
25 IF (YN .GT. YF) YF=YN
IF (YC .LT. Y1) Y1=YC
26 CONTINUE
YC=Y1
YN=YF
FIRSTV=YC
IF (YC) 34,35,35
34 FAD=FAD-1.0
35 DELTAV=(YN-FIRSTV)/AXLEN
IF (DELTAV) 70,70,40
40 I=ALOG10(DELTAV)+1000.0
P=10.0**(1-I000)
DELTAV=DELTAV/P-0.01
CC 45 I=1,6
IS=I
IF (SAVE(I)-DELTAV) 45,50,50
45 CONTINUE
50 DELTAV=SAVE(IS)*P
FIRSTV=DELTAV*AINT(YC/DELTAV+FAD)
T=FIRSTV+(AXLEN+0.01)*DELTAV
IF (T-YN) 55,57,57
55 FIRSTV=P*AINT(YC/P+FAD)

```

```
T=FIRSTV+(AXLEN+.01)*DELTAV
IF (T-YN) 56,57,57
56 IS=IS+1
   GC TO 50
57 FIRSTV=FIRSTV-AINT((AXLEN+(FIRSTV-YN)/DELTAV)/2.0)*
  1DELTAV
   IF (Y0*FIRSTV) 58,58,59
58 FIRSTV=0.0
59 IF (INC) 61,61,65
61 FIRSTV=FIRSTV+AINT(AXLEN+.5)*DELTAV
   DELTAV=-DELTAV
60 FIRST=FIRSTV
   DEL=DELTAV
67 RETURN
70 DELTAV=2.0*FIRSTV
   DELTAV=ABS(DELTAV/AXLEN)+1.
   GC TO 40
   END
//GC.PLOT01 DD DSN=ME48.GATER,
// DISP=(NEW,CATLG),UNIT=PLOTDISK,
// DD=PLKSIZE=1000,SPACE=(CYL,8,RLSE),LABEL=RETPD=2
//GC.FT10FC01 DD DSN=ME48.BINGO,DISP=SHR,UNIT=TAPE
//GC.SYSIN DD *
/*
```

APPENDIX II

VERIFICATION OF THE COMPUTER CODE

The following test cases were used to show that the Thrust Malalignment Computer Code will give accurate results in the prediction of motion about a fixed point. Each case was solved by an exact analytical technique and also by the computer. The results of each method of solution are indicated.

Test-1

Calculation of the Period of Motion of a Simple Pendulum in a Gravitational Field

Consider a simple pendulum as shown in Figure 29. Mass m is a fixed distance l from the pivot point O in coordinate system xyz . XYZ is the inertia reference frame. θ_0 and ψ_0 are the original nutation and precession angles. The pendulum is released in a gravitation field with an acceleration vector in the $-Z$ direction. $\bar{T} = -l\bar{e}_z$. The problem is to study $\theta[T]$ using the computer program for a single case of θ_0 , ψ_0 . The period of motion for the pendulum will be compared to the standard solution for the problem.

Standard Solution

The exact solution may be obtained as follows [3]:

$$T = 4 \sqrt{\frac{l}{g}} K(k)$$

where,

$$K(k) = F\left(\frac{\pi}{2}, k\right) \quad \text{complete elliptic integral of the first kind.}$$

$$k = \sin \frac{\theta_0}{2}$$

$$K(k) = \int_0^{\pi/2} \frac{d\phi}{\sqrt{1 - k^2 \sin^2 \phi}}$$

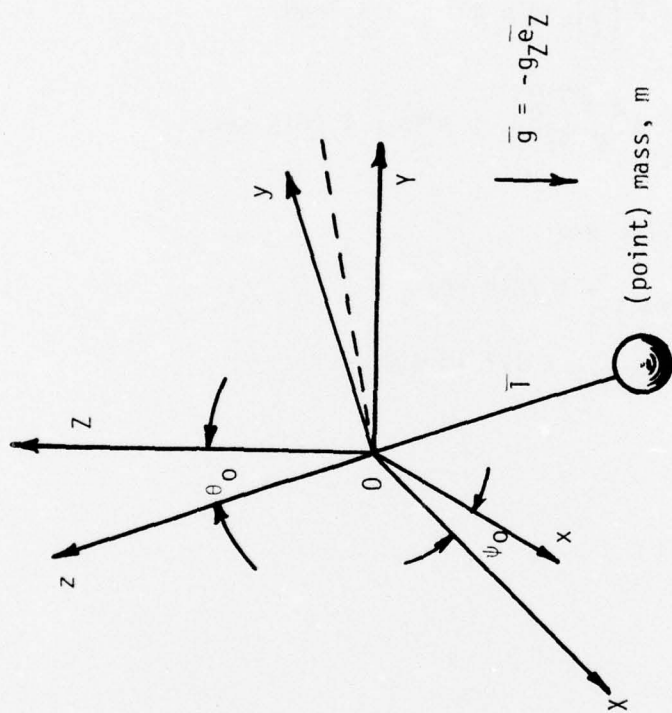


Figure 29. A Simple Pendulum Oscillating in a Gravitation Field

Consider a pendulum with the following characteristics:

$$g = 32.1 \text{ ft/sec}^2$$

$$\psi_0 = 0.0^\circ$$

$$m = 1.0 \text{ slug}$$

$$\theta_0 = 80.0^\circ$$

$$w = 32.1 \text{ lbs}$$

$$I = .0001 \text{ slug-ft}^2$$

$$l = 1.0 \text{ ft}$$

$$I' = 1.0 \text{ slug-ft}^2$$

$$K(k) = F\left(\frac{\pi}{2}\right), \sin 40^\circ = 1.7868$$

$$T = 4 \sqrt{\frac{1.0}{32.1}} 1.7868 = 1.2615 \text{ sec.}$$

The final results are:

$$T_{\text{exact}} = 1.2615 \text{ sec}$$

$$T_{\text{computer}} = 1.2618 \text{ sec}$$

Test-2

Spinning Gyroscope in a Gravitational Field

Consider the problem of determining the motion of a spinning gyroscope in a gravitational field as shown in Figure 30. The gyroscope is a 1 in. thick, 6 in. diameter steel disk mounted midway along a 12 in. spindle. The spindle's spin axis is always coincident with the z axis in xyz. The inertia reference is the XYZ coordinate set.

Find:

the rate of precession, $\dot{\psi}$

the nutation amplitude, θ_{AMP}

the nutation period, T_{θ}

where,

$$\dot{\theta}_0 = 7500 \text{ rpm} = 785.398 \text{ rad/sec}$$

$$\psi_0 = 0^\circ$$

$$\theta_0 = 15^\circ$$

$$l = .5 \text{ ft}$$

$$r = .25 \text{ ft}$$

$$h = .0833 \text{ ft.}$$

$$m = 2 \text{ slugs}$$

$$g = 32.16 \text{ ft/sec}^2$$

$$I = \frac{mr^2}{2} = .0625 \text{ slug-ft}^2$$

$$I' = \frac{m(12l^2 + 3r^2 + h^2)}{12} = .5324 \text{ slug-ft}^2$$

$$w = 64.32 \text{ lbs}$$

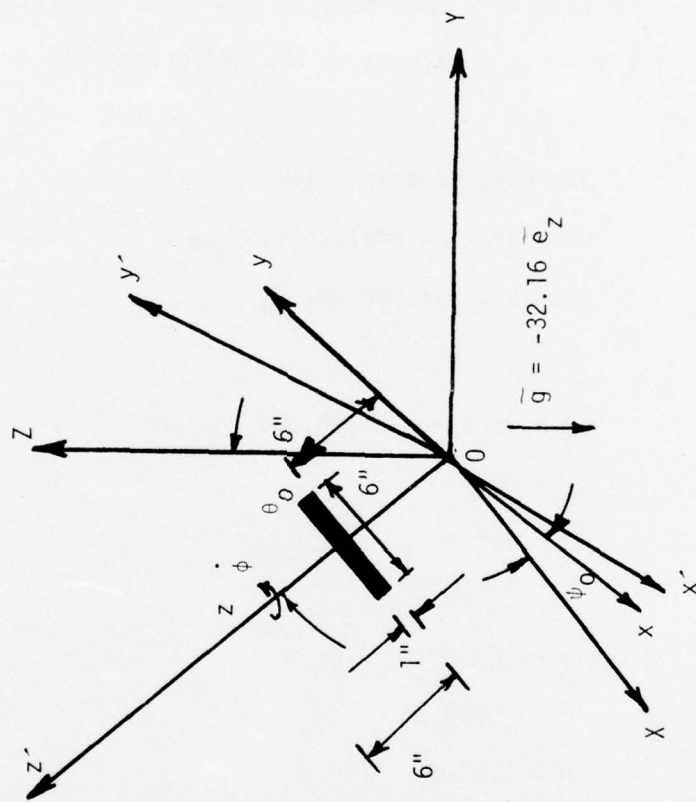


Figure 30. Spinning Gyroscope in a Gravitational Field

The results of the computer solution compare with the exact solution as follows:

	COMPUTED SOLUTION	EXACT SOLUTION*
Nutation Period	.069 sec/cycle	.068 sec/cycle
Nutation Amplitude	.00378 radians	.00374 radians
Precession Rate	.642 rad/sec	.655 rad/sec

* SEE REFERENCE [4].

REFERENCES

1. Shames, I. H., Engineering Mechanics-Dynamics, Prentice-Hall, Inc., Englewood Cliffs, New Jersey, (1966).
2. Meriam, J. L., Dynamics-2nd Edition, John Wiley and Sons, Inc., New York, (1971).
3. Greenwood, D. T., Principles of Dynamics, Prentice-Hall, Inc., Englewood Cliffs, New Jersey, (1965).
4. Scarborough, J. B., The Gyroscope, Theory and Applications, Interscience Publishers, New York, (1958).